A Szilikátipari Tudományos Egyesület lapja

építőanyag

Journal of Silicate Based and Composite Materials

A TARTALOMBÓL:

2020/1

TURKEYTRIB 2020 3rd INTERNATIONAL CONFERENCE ON TRIBOLOGY

June 18-20 2020

CONFERENCE VENUE: Elite World Prestige Hotel
ADDRESS: Şehit Muhtar Caddesi No:40, 34435 Taksim Istanbul-TURKEY
WELCOME TO TURKEYTRIB 2020!

We are very pleased to announce that the 3rd International Conference on Tribology TURKEYTRIB 2020 will be held from 18 to 20 June 2020 at the Elite World Prestige Hotel Taksim-İstanbul-TURKEY. The scope of this conference embraces the state of art and future trends in tribology research and application, emphasizing the necessity of facilitation intellectual collaboration across both disciplinary and national-international boundaries. The main objective of the conference is to provide a unique opportunity of presenting and discussing recent developments in different aspects of Tribology and strengthen the linkage between academia and industry. The conference consists of scientific sessions, symposia on specific topics, exhibitions and various collateral events. Turkish and Foreign groups of experts will have chance to share information and get in touch with other groups in all part of Tribology. Nowadays these aspects are becoming more and more important both in respect of human life and environment.

– SPECIAL ISSUE (Web of Science Core Collection-Emerging Sources Citation Index): Selected high-quality papers (10) presented at the TurkeyTrib'20 conference will be selected and invited to submit their contributions for Special Issue publication in Építőanyag - Journal of Silicate Based and Composite Materials. (SCIE; Impact Factor 1.079 (2018). The submission due is 30 June 2020.

www.turkeytribconference.com/index.php/en/

TURKEYTRIB 2020
3rd INTERNATIONAL CONFERENCE TRIBOLOGY
18-20 JUNE
ELITE WORLD PRESTIGE HOTEL-TAKSIM
ISTANBUL-TURKEY

építőanyag

Journal of Silicate Based and Composite Materials

2020/1

TARTALOM

CONTENT

A finomkerámia-, üveg-, cement-, mész-, beton-, tégla- és cserép-, kő- és kavics-, tűzállóanyag-, szigetelőanyag-iparágak szakmai lapja
Scientific journal of ceramics, glass, cement, concrete, clay products, stone and gravel, insulating and fireproof materials and composites

A folyóiratot referálja · The journal is referred by:
ProQuest · Google Scholar · Index Copernicus International · Thomson Reuters

A folyóiratban lektorált cikkek jelennek meg.
All published papers are peer-reviewed.
Kiadó · Publisher: Szilikátipari Tudományos Egyesület (SZTE)
Elnök · President: ASZTALOS István
1034 Budapest, Bécsi út 122–124.
Tel.: +36-1/201-9360 ▪ E-mail: epitoanyag@szte.org.hu
Tördelő szerkesztő · Layout editor: NÉMETH Hajnalka
Címlapfotó · Cover photo: GYURKÓ Zoltán

Hirdetési árak 2020 ▪ Advertising rates 2020:

B2 borító színes · cover colour	76 000 Ft	304 EUR
B3 borító színes · cover colour	70 000 Ft	280 EUR
B4 borító színes · cover colour	85 000 Ft	340 EUR
1/1 oldal színes · page colour	64 000 Ft	256 EUR
1/1 oldal fekete-fehér · page b&w	32 000 Ft	128 EUR
1/2 oldal színes · page colour	32 000 Ft	128 EUR
1/2 oldal fekete-fehér · page b&w	16 000 Ft	64 EUR
1/4 oldal színes · page colour	16 000 Ft	64 EUR
1/4 oldal fekete-fehér · page b&w	8 000 Ft	32 EUR

Az árak az áfát nem tartalmazzák. · Without VAT.

A hirdetési megrendelő letölthető a folyóirat honlapjáról.
Order-form for advertisement is avaliable on the website of the journal.

WWW.EPITOANYAG.ORG.HU
EN.EPITOANYAG.ORG.HU

Online ISSN: 2064-4477
Print ISSN: 0013-970x
INDEX: 2 52 50 ▪ 72 (2019) 1–38

Strengthening of masonry walls with CFRP composite: experiments and numerical modeling

Houria HERNOUNE ▪ Department of Civil Engineering, University Yahia Fares, Algeria
Benchaa BENABED ▪ Civil engineering laboratory, University of Amar Telidji, Algeria
Madyan ALSHUGAA ▪ Department of Civil Engineering, University King Fahd University of Petroleum and Minerals, Saudi Arabia
Rajab ABOUSNINA ▪ Centre for Future Materials, School of Civil Engineering and Surveying, University of Southern Queensland, Australia
Abdelhamid GUETTALA ▪ Department of Civil Engineering, University Mohamed Khider, Algeria

Érkezett: 2019. 12. 26. ▪ Received: 26. 12. 2019. ▪ https://doi.org/10.14382/epitoanyag-jsbcm.2020.1

Abstract

The paper presents the experimental and numerical study of brick masonry walls reinforced with carbon fiber-reinforced polymer (CFRP) composite subjected to a shear load. In this analysis the Concrete Damaged Plasticity (CDP) constitutive laws are utilzed to simulate the non-linearities in the behavior of brick and mortar. These models are used for the analysis of diagonal compression tests on masonry panels. The experimental results are used to validate the modelling approach presented here. The results showed that the application of the CFRP composite on unreinforced masonry (URM) has a great influence on strength, post-peak behavior, as well as changing failure modes and ductility. On the other hand, the adopted detailed micro-modelling approach (DMM) gives a good interface for predict the shear response on masonry walls.

Keywords: masonry walls, CFRP composites, shear loads, detailed micro-modelling approach, diagonal compression tests
Kulcsszavak: téglafalazatok, CFRP kompozitok, nyírás, részletes mikro-modellezési eljárás, átlós nyomószilárdság teszt

Houria HERNOUNE
Lecturer at the Department of Civil Engineering, University of Medea, Algeria, Her research interests include Strengthening of masonry walls with CFRP composite, analytical modelling and simulation.

Benchaa BENABED
PhD, Associate professor at the Department of Civil Engineering, University of Laghouat, Algeria. His research interests include, self-compacting concrete, reuse of local materials, rheology and durability of cement-based materials. *Corresponding author. E-mail: b.benchaa@lagh-univ.dz

Madyan ALSHUGAA
PhD student at University King Fahd University of Petroleum and Minerals,Dhahran, Saudi Arabia. His research interests include Strengthening of masonry walls with CFRP composite, analytical modelling and simulation

Rajab ABOUSNINA
PhD, Research fellow and teaching assistance, in School of Civil Engineering and Surveying, University of Southern Queensland, Australia. His principal research interests focus on concrete technology, waste materials, geopolymer concrete, analytical modelling and simulation.

Abdelhamid GUETTALA
Professor at the Department of Civil Engineering, University of Biskra, Algeria. His research interests include, concrete technology, reuse of local materials.

1. Introduction

Around the world, there are many old unreinforced masonry (URM) structures such as historical cultural monuments and bridges, etc. which are deteriorated or damaged during earthquake events [1, 2]. In order to extend the life of such structures, strengthening or repairing by implementing new techniques have been developed. Many of these strengthening techniques including the use of fiber reinforced polymer (FRP) composites were used to reinforce masonry structures. These composites are manufactured in different features depending on the fiber material type like carbon fiber (CFRP), glass (GFRP), and aramid (AFRP). FRP strips offer the possibility of application by gluing on the outside surface EB (externally bonded) or inserting inside the groove of element by the near-surface mounted (NSM)technique. The use of FRP composites embedded into polymetric matrix such as (polyester, epoxy, mortar mix) can be the perfect solution for retrofit the structure walls in seismic area. The application of FRP composite to strengthen and rehabilitate masonry has been studied by several authors. Experimental studies evaluate the effect of different variables for example, the effect of retrofitting configuration of FRP composite, type of FRP composites and the type of masonry components, through small-scale testing such as triplets test, Wallette and by full scale testing. Mahmood and Ingham [3] conducted a series of experimental test on URM walls, they illustrated the effectiveness of FRP retrofitting system in improving the shear strength of unreinforced masonry with a factor of 3.25. Valluzzi et al [4] tested a series of unreinforced brick masonry panels strengthened by different materials (GFRP, CFRP and PVAFRP) of different configuration. All tested specimens were subjected to a diagonal compression test, the results showed that the application of FRP at one side of the wall only produces a significant out-of-plane deformation, corners and the failure mode of the out-of-plane displacement exaggerated by the little restraint at the top and bottom of the wall. Several researchers such as Haroun et al [5], Tumialam et al [6], Hamid et al [7] and Li et al [8] have shown that FRP composites can improve the shear capacities of URM walls significantly. All these experimental studies have shown that the use of FRP strengthening technique can ensure adequate increase of seismic capacity, stiffness and ductility of masonry wall in the in plane lateral loading [9,10] or out-of-plane [11].

To understand the structural behavior of the masonry wall during earthquakes, it is significant to model this using advanced technique. In the literature two major approaches have been developed for masonry modeling namely heterogeneous and homogeneous modeling. In the first approach the brick units and joint mortar are considered separately (heterogeneous modeling). While, in the second approach (homogeneous modeling) the brick units, joint mortar and interfaces between them are assumed to be either an isotropic or anisotropic composite material. According to the classification of Lourenco (1995) [12] there are two main modelling approaches: macro-modelling and micro-modelling (see *Fig.1*). The micro-modeling can be divided into two techniques as detailed micro-modeling and simplified micro modeling [13].

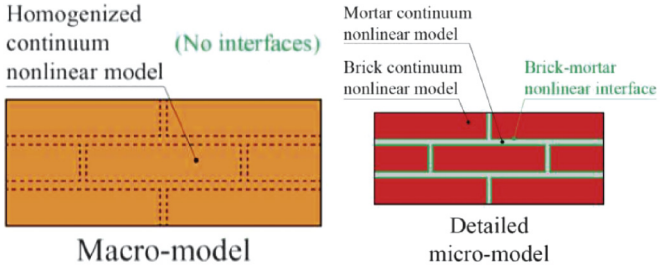

Fig. 1 Modelling strategies for masonry structures
1. ábra Falazott szerkezetek modellezési stratégiái

In the detailed micro-modeling (see *Fig. 1b*) each component (units and mortar) is modeled separately with unit-mortar interface. The concept of micro modeling is adopted for analysis in detail of small masonry structural elements such as masonry shear triplets or small panel wall . In this approach the masonry units and mortar are modelled with real thickness, while zero thickness is assigned to unit-mortar interfaces. The units and mortar are modelled as continuum elements and unit-mortar interfaces are modelled as discontinuous elements.

The literature has been clearly focused on the importance of including all mechanisms of rupture of the masonry in the modeling to understand its behavior, in terms of ductility and ultimate load as well as the damage which is usually concentrated at the mortar interface [14,15]. In microscopic models, only a tensile breaking of the bricks is sometimes considered, most studies relying only on a linear elastic behavior of the bricks. Or in other words, the authors adopted this model assent to the need to introduce the post-peak softening behaviors of the mortar. The progressive cracking of the elements must be reproduced by the softening in tension. In shear, the degradation of the cohesion and that in compression leads to the crushing of the masonry. The softening behavior laws, which are thus essential in modeling, however, rely on the definition of many parameters whose values are difficult to be predicted. This modeling is therefore only feasible if it is coupled with a several experimental test for best description of the material and their interactions.

In the present study, the influence of the type of joint mortar and location of the CFRP composites in the strengthened panels subjected to shear loads is evaluated by diagonal compression test. For the numerical analysis, a numerical model based on the DMM approach was developed using FE software ABAQUS and validate with the experimental data. The result of these numerical examples is compared with the experimental result.

2. Experimental program

The test consists of testing four unreinforced walls (control panels noted MT) and six walls reinforced with CFRP composites in order to evaluate the reinforcement efficiency and the mode of rupture in case of each reinforcement.The reinforced panels were strengthened by Sika Warp carbon fiber CFRP composites of 50 mm width. The FRP reinforcement was glued, using two-part epoxy adhesive. Three configurations of the retrofit system were investigated.

2.1 Materials

2.1.1 Brick units

The perforated bricks were tested in compression and in bending. Five test series has been studied to obtain the average values of compressive strength and the elastic modulus. The tests were carried out using a hydraulic press according to the EN 771-1 [16].

2.1.2 Cement-Lime mortar

The cement-lime mortars are commonly adopted, because these mortars have the good properties of cement as well as lime mortars, that is, medium strength along with good water retentively, good workability and to some extent freedom from cracks. Therefore, this type of mortar has been adopted.

Two mixes consisting of cement: lime: sand proportions (1:1:3 and 1:1:5) were prepared using an electrical mixer by weight batching. Water was added and the mixture was remixed to achieve a workable consistency. In order to measure the mechanical properties of these mortars, the prepared mixtures were cast into standard molds and then maintained in the standard curing. The mechanical properties of mortars were determined at the age of 3, 7, 14 and 28 days after de-molding. Flexural and compressive strength tests were measured according to EN 1015-11 [17]. By using the universal testing machine, the flexural strength has been tested on specimens in the shape of a prism 40×40×160mm^3 . Afterward, the two half-prisms obtained after breaking into two parts from the specimen during the flexural test were subjected to the uniaxial compressive test (results are shown in *Table 1*). Six specimens of each mix are tested to have the average value of the response. The average values of the brick compressive strength, the mortars compressive strength and secant modulus of elasticity are reported in *Table 1*.

Material	Compressive strength (MPa)	Flexural strength (MPa)	Young's modulus (MPa)
Mortar A (1:1:3)	7.187	3.341	3639.24
Mortar B (1:1:5)	3.643	1.453	1880.87
Brick	20.53	_	1.E+04

Table 1 Compressive strength, flexural strength and young modulus of mortar and brick
1. táblázat A habarcs és tégla nyomószilárdsága, hajlítószilárdsága és rugalmassági modulusa

2.1.3 Composite materials (SikaWrap carbon fiber)

In this study, a unidirectional carbon fibre (Sika Wrap carbon fiber fabric) is employed. The technical characteristics are summarized in the following *Table 2*.

Property	Value
CFRP width	300 / 600 mm
CFRP length / roll	≥ 50 m
Weight	235 g/m^2 ± 10 g/m^2
Thickness	0.129 mm
Density (Fiber)	1.82 g/cm^3
E_{CFRP}	230 kN/mm^2
Ft_{CFRP}	4000 N/mm^2
Rupture strain	1.70%

Table 2 Mechanical properties of the CFRP reinforcing system (nominal values reported by the manufacturer)
2. táblázat A CFRP mechanikai tulajdonságai (gyártó által közölt névleges értékek)

2.2 Methods

The test specimens were made according to the instructions given in RILEM technical recommendation [18]. A series of ten masonry wallettes were constructed from perforated brick with dimensions 220 × 105 × 55 mm³ and mortar joint with 10 mm of thickness. Two types of mortar (type A, type B) were used in the construction of the panels having mix ratio of 1:1:3 and 1:1:5 of (Portland cement: hydrated lime: sand). The test involves subjecting a square section of masonry, with global dimensions 400 × 400 × 105 mm³, to a compressive load applied along the diagonal. The experimental setup for the diagonal compression test is presented in *Fig. 2*.

Fig. 2 Experimental setup of unreinforced masonry panels tested in diagonal compression
2. ábra Kísérleti összeállítás megerősítetlen falazat diagonális nyomószilárdság vizsgálatára

The walls are placed and centered diagonally between the two plates of the press with the help of the metal shoes. These allow the transmission of the load to the wall in the vertical direction. The load is applied using the hydraulic cylinder which is placed below the load cell. The measurement of displacements is carried out using two displacement sensors which are installed on the diagonal of the wall. All data, forces and displacements, are automatically recorded by a data acquisition system, and given automatically by the system. The loading is applied by a machine of capacity 500 kN. The loading speed is 5 mm/min.The tests were performed under displacement control in order to obtain the complete stress-strain curve of the panels. All tested wall panels were of similar dimensions in order to permit direct comparison of their failure loads (see *Figs. 3*, *4*).

Fig. 3 Specimen preparations of unreinforced masonry panels
3. ábra Megerősítés nélküli falazat minták előkészítése

The shear strength is calculated according to the state of stress in the center of the wall; isotropic or anisotropic. The calculation of the shear stress τ_{dt} is made according to ASTM 519 - 02[19]. considering a state of isotropic stress in the center of the wall.

$$\tau_{dt} = \frac{P_{max}}{\sqrt{2} \times A} \quad (1)$$

The lateral surface A is subjected to a maximum load P_{max} Area A is calculated with Equation (2) by considering w width, h height and t wall thickness.

$$A = \frac{w+h}{2} \times t \quad (2)$$

The displacement ductility factor (μ) is defined as the ratio between the ultimate displacement to the yield displacement:

(3)

δ_u : displacement at ultimate load

δ_y : displacement at the load causing yield condition

The shear modulus G is calculated in the zone of elastic stress with Equation (4)

$$G = \frac{\Delta\tau_e}{\Delta\gamma_e} \quad (4)$$

$\Delta\tau_e$ and $\Delta\gamma_e$ represent stress and elastic strain, respectively.

Fig. 4 Specimen preparations and configuration of reinforcing for masonry panels
4. ábra Megerősített falazat minták előkészítése

3. Experimental results and discussion

3.1 Behavior of control walls

In wall panels MTA and MTB cracking occurred predominately through the mortar joints in a diagonal, followed by a rapid decrease in load capacity. With load increasing, the wall exhibited a gradual increase in the width of predominately diagonally oriented crack,with further increase in load multiple cracks were observed in the panel before failure as shown in *Fig. 5*. The MTA control wall has a maximum shear strength of 0.5 MPa corresponding to a maximum force of 33.66 kN. In addition, the MTB wall has a breaking force of 35.06 kN, which produces in this wall a maximum shear stress of 0.56 MPa (see *Table 3*). The shear stress-strain response of the tested unreinforced wall panels (MTA and MTB) is summarized in *Fig. 7*. For a comparison between the two responses, The wall panel constructed with mortar A failed at lower load compared to the wall panel type B,but with a slight difference. Both MTA and MTB wall panels exhibited an approximately linear shear stress-strain response until cracking, for the wall MTA followed by rapid degradation of shear strength once cracking propagated, but for wall MTB followed by a slight increase in shear strength and deformation capacity before the rupture.

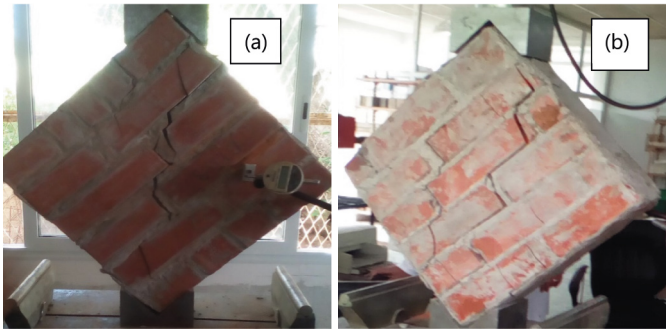

Fig. 5 Failure modes of control masonry panels: (a) MTA, (b) MTB
5. ábra A referencia falazat panelek tönkremeneteli módjai

3.2 Reinforced masonry panels subjected to the diagonal compression

In unreinforced walls, the tensile stress causes an appearance of cracks leading to a complete destruction. However, in the case of walls strengthened with CFRP composites, the tensile stresses are transferred to these strips and it results in a significant reduction of stress in the masonry wall. Regarding the overall response of the walls, the results obtained revealed a significant increase in shear stress from 65% to 270% compared to unreinforced walls. Likewise, it was found that the improvement in ductility for strengthened wall panels type A ranged from 74% to 80% ,whereas for wall panels type B it ranged between 80% to 88% (see *Table 3*). The CFRP reinforced panel failed suddenly due to a cracking along the compressed diagonal at the ends of the composite strips (see *Fig. 6*). The MRX and MRH walls have a maximum force of 55.27 kN and 57.58 kN respectively, which is a value of 1.82 MPa and 1.85 MPa for shear strength. and present better shear behavior with increase of 200%. This reinforcement allowed to increase the ductility μ up to 88%. Thus, when the joint of the mortar cracks, there is a redistribution of the force towards the part of the reinforcement which is in the vicinity of the crack. Therefore, the arrangement of the reinforcing composites has a very important effect on the local behavior of the structure, due to the stress distribution and the deformation of the structure. An application of CFRP composite on a 24% wall surface sufficient to increase wall ductility, and give almost the same results as that recorded when the fabric covers an area of 54 and 56%. The first conclusion, which can be obtained from the experimental results, is that the wall panels reinforced by CFRP composite technique presented more ductile behavior compared with the control wall panels for each type of mortar (see *Fig. 7*). Moreover, the shear strength of reinforced wall panels is dependent on the mortar resistance.

panels	type	fiber	F_{max} (kN)	τ (MPa)	G (MPa)	γ_e	γ_u	μ	(μ_u/μ_o)
MT	A	0%	33.66	0.50	77	0.023	0.027	1.16	——
	B	0%	35.063	0.56	78	0.029	0.031	0.94	——
MRH	A	54.68%	54.958	1.76	92	0.056	0.111	2.02	73.98
	B	54.68%	57.583	1.85	80	0.033	0.058	1.74	85.06
MRX	A	54.06%	50.815	1.61	117	0.027	0.057	2.1	80.87
	B	54.06%	55.274	1.82	128	0.028	0.049	1.78	88.83
MRI	A	22.91%	50.455	1.59	113	0.021	0.039	1.90	64.09
	B	22.91%	45.607	1.45	103	0.021	0.036	1.80	80.00

γ_e: Elastic deformation – γ_u: Maximum deformation at ultimate load – μ: ductility factor – (μ_u/μ_o): improvement between unreinforced and reinforced masonry walls – *fibers (%)*: percentage occupation of the surface walls by carbon fiber band

Table 3 Ultimate shear strength and ductility factors for experimental tests of unreinforced and reinforced wall
3. táblázat A megerősített és megerősítés nélküli falazatok nyírószilárdsága és duktilitási tényezői

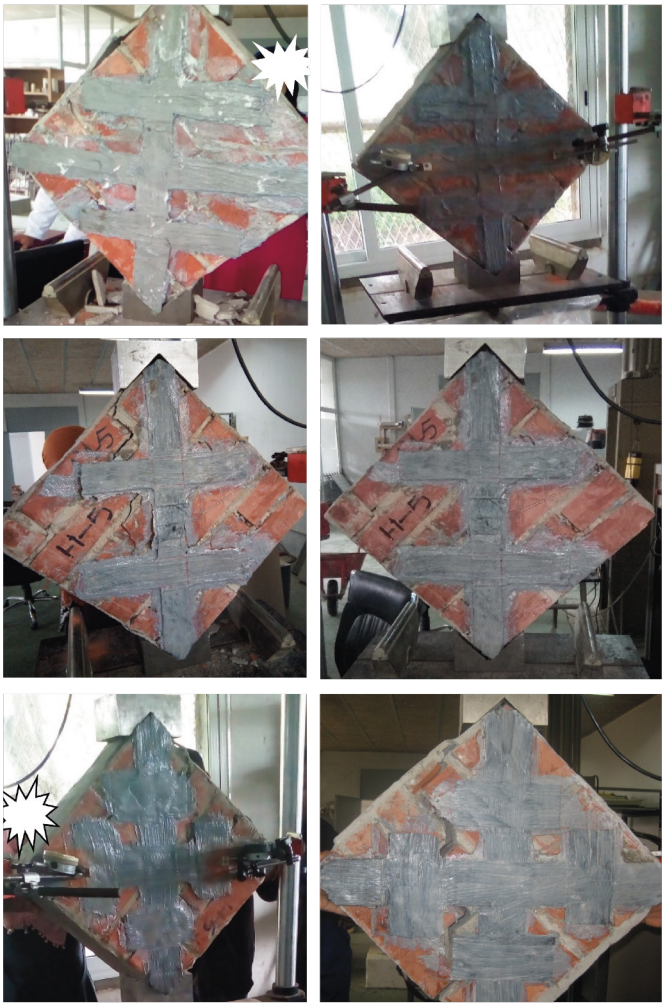

Fig. 6 Failure modes of all strengthened masonry panels: (a) MHA and MHB, (b) MIA and MIB, (c) MXA and MXB
6. ábra Megerősített falpanelek tönkremeneteli módjai: (a) MHA és MHB, (b) MIA és MIB, (c) MXA és MXB

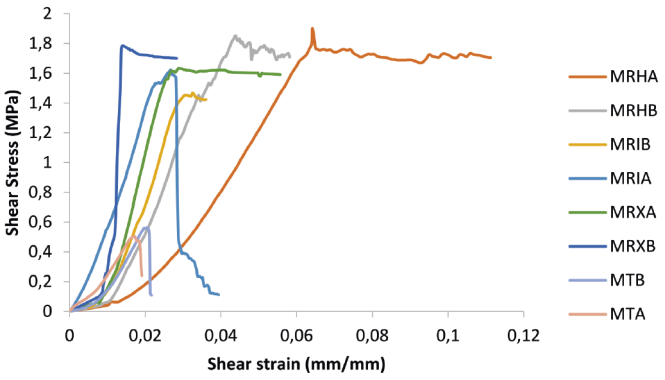

Fig. 7 Shear stress-strain relationship for unreinforced and reinforced masonry panels
7. ábra Nyírófeszültség-alakváltozás összefüggése megerősítés nélküli és megerősített falpanelek esetén

4. FEM modeling for unreinforced masonry wall (MTB)

4.1 Material parameters

In this study, the FE software, ABAQUS was used to evaluate the validity of proposed model (DMM) approach for predicting behavior of brick masonry wall. The units and mortar joints are modelled using eight noded 3D continuum elements with hour glass control and reduced integration (C3D8R), and the unit-mortar interface with zero thickness. The penalty friction formulation was introduced to model tangential behavior with a friction coefficient value of 0.6. The normal behavior of the interface was modeled using "hard contact", the nonlinear behavior of brick and mortar was simulated by using the CDP model. The interface between unit and mortar was modeled through surface-to surface contact. The adopted modeling strategy used in this study is illustrated in *Fig. 8*.

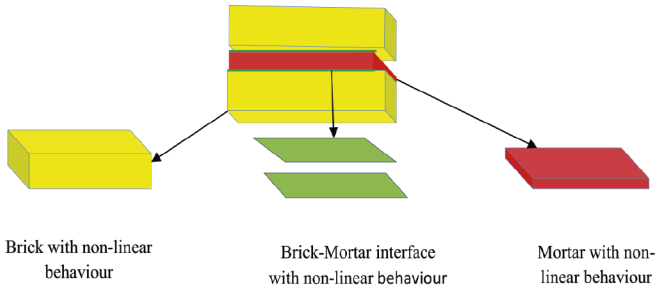

Fig. 8 Adopted detailed micro-modeling (DMM) approach
8. ábra Részletes mikro-modellezési megközelítés

4.2 Presentation of the numerical model

To validate the model proposed in this study, the same wall that which was studied in the experimental part was chosen (MTB). *Fig. 9* shows the geometry and loading condition for the FE model that has been implemented using ABAQUS.

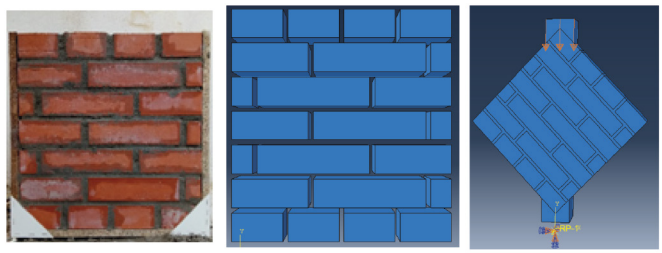

Fig. 9 Numerical model (DMM) and boundary conditions of unreinforced brick masonry wall
9. ábra Numerikus modell és peremfeltételei megerősítés nélküli falazat esetén

4.3 Constitutive behavior of units and mortar

4.3.1 Concrete damage plasticity (CDP) model

The Concrete damage plasticity (CDP) model provides a general capability for modeling concrete and other quasi-brittle materials. This model which was developed by Lubliner et al (1989) [20] and adopted by Abaqus is selected in this study to simulate the nonlinear behavior of the masonry units. This approach has been developed to predict the two main masonry failure mechanisms such as cracking under tension and crushing under compression. The CDP model uses the concepts of isotropic damaged elasticity in combination with isotropic tensile and compressive plasticity [21]. The level of damage is represented by damage parameters d_c and d_t as shown in *Figs. 10* and *11*.

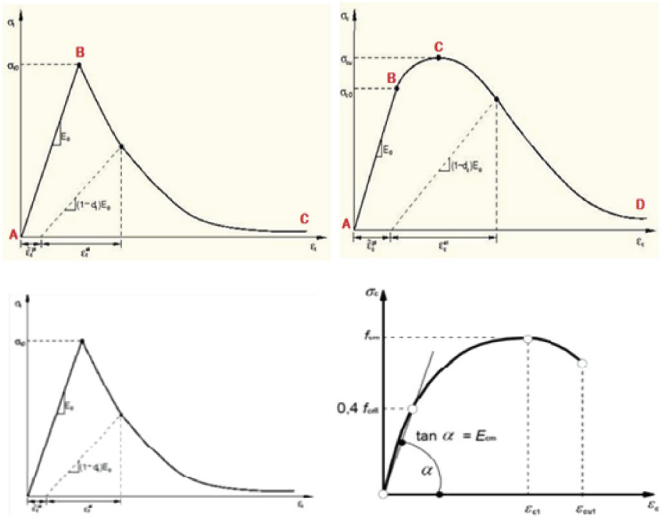

Fig. 10 Brick and mortar response to uni-axial loading; (a) Brick: in tension and compression; (b) Mortar: in tension and compression [19]
10. ábra Tégla és habarcs viselkedése egytengelyű terhelés hatására: (a) tégla: húzás és nyomás; (b) Habarcs: húzás és nyomás [19]

4.3.2 Constitutive behavior of units-mortar interface

In this model, brick–mortar interface is modeled by means of Coulomb friction criterion, in order to adequately reproduce the shear response of joint, the values of cohesion and friction angle for a Coulomb type friction model are provided by the envelop of the shear strength for different normal stress values, which was obtained experimentally by the triplet test (see *Fig. 12*). The interaction module of Abaqus/Explicit analysis was used to make the contact between units and mortar through the option surface-to surface contact. In this step it is necessary to define two contact properties: normal contact and tangential behavior.

4.4 Model input parameter

In this section, the input parameters used to reproduce the mechanical behavior of masonry wall using the detailed micro-modeling approach is presented. The mechanical parameters for brick and mortar employed in this analysis were obtained from tests carried out in this research (see *Tables 4*, *5*).

Elasticity parameters	Brick	Mortar
Mass Density γ (kg/m³)	2200	1800
Young's modulus (MPa)	10000	1880
Poisson ratio ν	0.2	0.18

Table 4 Mechanical properties of masonry unit and mortar
4. táblázat A habarcs és a falazat mechanikai tulajdonságai

Plasticity parameters	
Dilation angle **Ψ** (°)	20
Eccentricity parameter e	0.1
Biaxial and unidirectional initial compressive strength ratio	1.16
Stress ratio in tensile meridian **K**	0.67
Viscosity Parameter	0.0001

Table 5 Concrete damage plasticity of masonry brick and mortar
5. táblázat A falazat képlékenyedési paraméterei

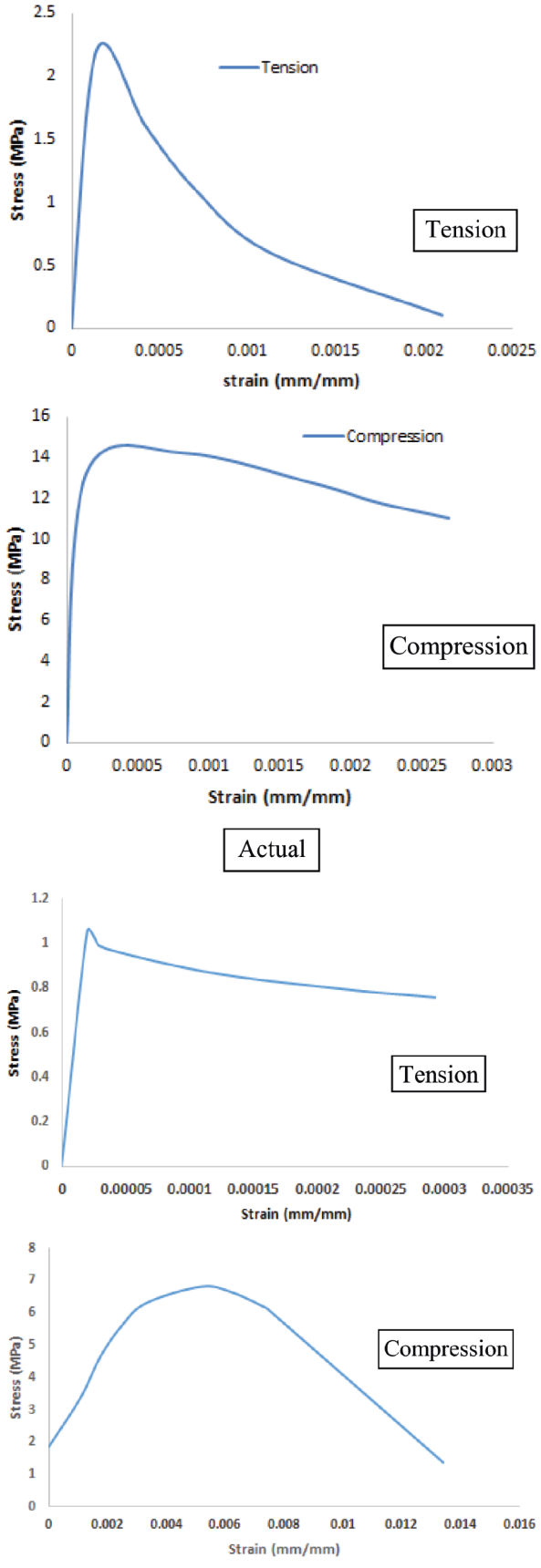

Fig. 11 Brick and mortar response to uni-axial loading; (a) Brick: in tension and compression; (b) Mortar: in tension and compression (present work)
11. ábra Tégla és habarcs viselkedése egytengelyű terhelés hatására: (a) tégla: húzás és nyomás; (b) Habarcs: húzás és nyomás (kísérletek alapján)

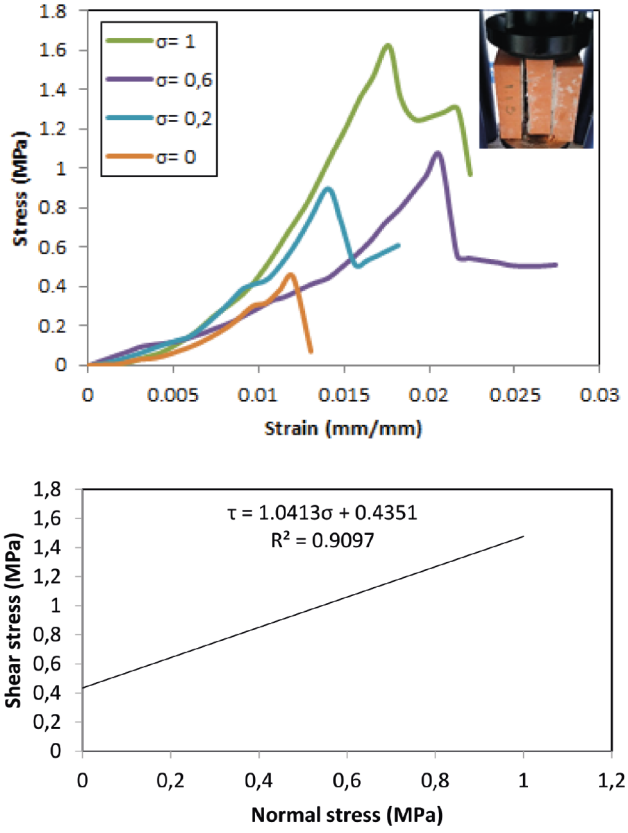

Fig. 12 *(a) Stress-strain curves for various precompression, (b) Relationship between maximum shear stress and normal stress*
12. ábra *(a) Feszültség-alakváltozás görbék különböző előkompresszió esetén, (b) Maximális nyíró és normal feszültség összefüggése*

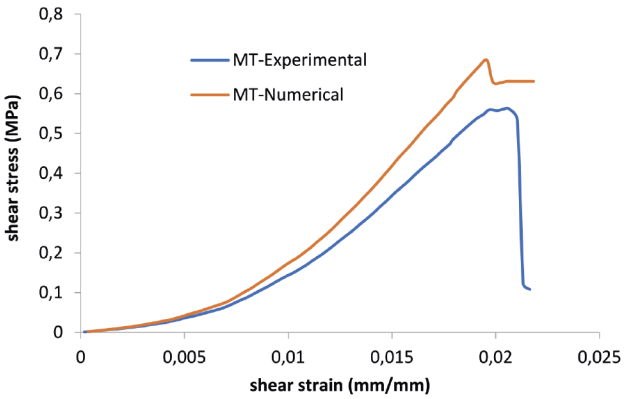

Fig. 13 *Confrontation of curves (σ – ε)*
13. ábra *Görbék összehasonlítása (σ – ε)*

The shear characteristics of the masonry and the brick/mortar joint interaction parameters at the interface are determined on a masonry prism (triplet), the test results of 16 triplets for confining stress varying from 0 to 1 MPa allowed us to determine the parameters shear strength and friction coefficient.

The shear strength (initial shear strength without any vertical stresses) is determined as follows:

$$\tau = \frac{P_{max}}{2A} \quad (5)$$

Where P is the shear load at failure and A is the cross-sectional area of contact between two bricks.

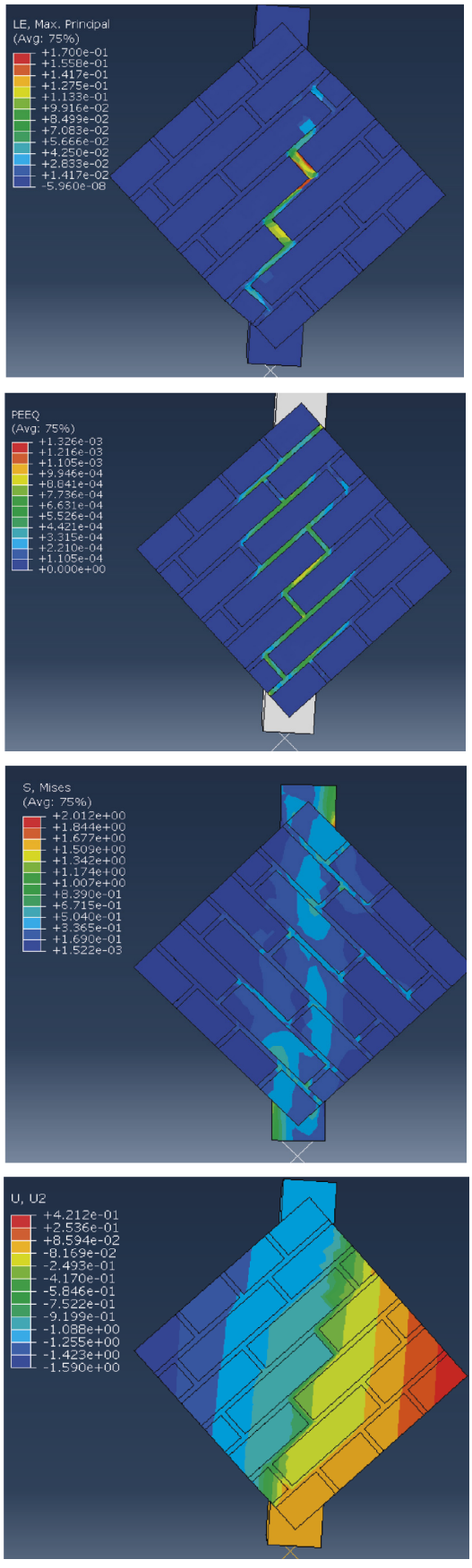

Fig. 14 *Von Mises stress distributions, deplacement in the direction y (U_{22}), plastic strain distributions (PEEQ) in the unreinforced brick masonry wall*
14. ábra *Von Mises feszültség eloszlás, y irányú elmozdulás (U_{22}), képlékeny alakváltozás (PEEQ) megerősítés nélküli tégla falazat esetén*

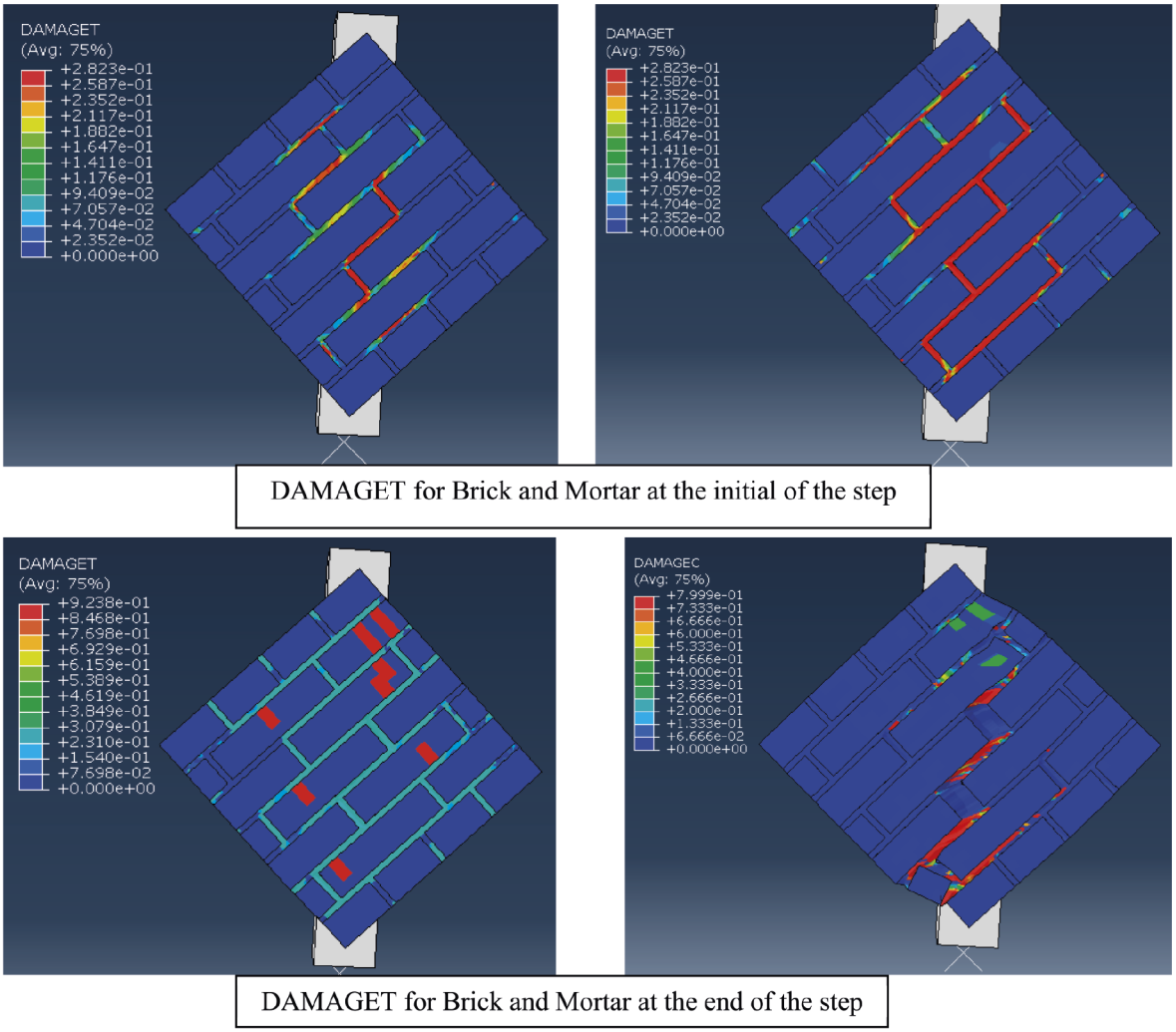

Fig. 15 Evolution of damage (DAMAGET, DAMAGEC) in the unreinforced brick masonry wall
15. ábra Tönkrementel kialakulása (DAMAGET, DAMAGEC) megerősítés nélküli falazatokban

The shear strength of the unit-mortar interface τ of masonry under normal stress was characterized through Coulomb failure criterion $\tau_u = c + \mu * \sigma_n$ (6)

Where $\mu = tan\varphi$ and c=τ_0 are the coefficient of friction and cohesion respectively.

The damage plasticity constitutive model was based on the following stress–strain relationship:

$$\sigma = (1 - d_t)\bar{\sigma}_t + (1 - d_c)\bar{\sigma}_c \quad (7)$$

where d_c and d_t were two scalar damage variables, ranging from 0 to 1.

the damaged parameter (d_c) is calculated by

$$d_c = 1 - \frac{\sigma_c}{\sigma'_c} \quad (8)$$

Where σ'_c is the compressive strength of masonry.

Damaged parameter (d_t) can be calculated by equation (9)

$$d_t = 1 - \frac{\sigma_t}{\sigma'_t} \quad (9)$$

where σ'_t is the masonry tensile strength

The uniaxial compressive and tensile responses of concrete with respect to the concrete damage plasticity model subjected to compression and tension load were given by:

$$\sigma_t = (1 - d_t)E_0(\varepsilon_t - \tilde{\varepsilon}_t^{pl}) \quad (10)$$

$$\sigma_c = (1 - d_c)E_0(\varepsilon_c - \tilde{\varepsilon}_c^{pl}) \quad (11)$$

the effective uniaxial stress σ_t and σ_c were derived as follows:

$$\bar{\sigma}_t = \frac{\sigma_t}{(1-d_t)}E_0(\varepsilon_t - \tilde{\varepsilon}_t^{pl}) \quad (12)$$

$$\bar{\sigma}_c = \frac{\sigma_c}{(1-d_c)}E_0(\varepsilon_c - \tilde{\varepsilon}_c^{pl}) \quad (13)$$

4.4 Comparison of results and discussion

The response obtained from the model is illustrated by the stress-strain diagram and by the damage of the panel. *Fig. 13* shows the numerical and experimental curves of the stress-strain relationship of unreinforced walls (MTB). The numerical results show a good agreement with the experimental results concerning not only at the initial rigidity of the elastic phase but also from the non-linear phase to the post peak response corresponding, but with a value from the numerical stress to the higher peak than the experimental value. Through these results show that the technique proposed in this study gives good results to analyzise the brick masonry wall behavior.

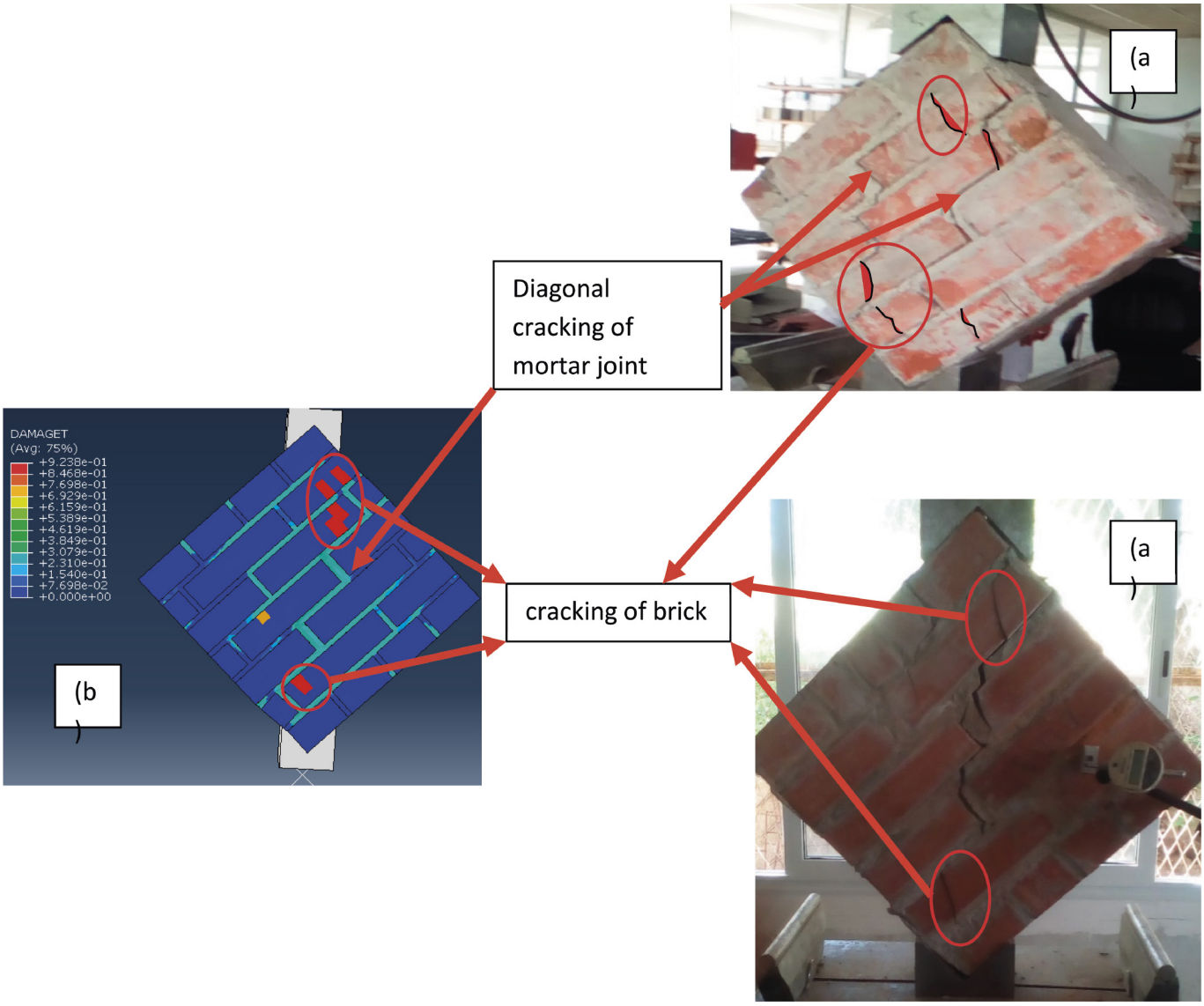

Fig. 16 Comparison between the numerical and experimental results concerning the crack pattern for the unreinforced wall MT: (a) experimental crack pattern; (b) numerical crack pattern

16. ábra Numerikus és kísérleti eredmények összehasonlítása a megerősítés nélküli MT falazat törésképét kiemelve: (a) kísérleti eredmény; (b) numerikus eredmény

4.4.1 Crack pattern and mode failure

Figs. 14 and 15 show the initial cracking occuring along the bed and head mortar joints in a diagonal (initial step). As the vertical loads increase, more cracks occur in the mortar joints of wall from top to down. After that, cracks appear and propagate in the brick directly in final step. Same mode of rupture was found experimentally.

Fig. 16 shows a comparison of the crack pattern developed in the numerical and experimental test for the masonry wall MTB. The crack patterns observed in the mortar joint and brick during the experiment test and predicted by FE model resemble each other to a good extent. A good correlation was found not only at the crack pattern of mortar but also from the brick. However, the position of cracks at the brick in numerical case differs from experimental test, this can be explained by the numerical simplification which consists in considering that all the mortar joints have the same thickness, the same mechanical characteristics, which is not assured experimentally.

5. Conclusions and future work

There is significant potential for the application of FRP in the masonry industry, both in the construction and rehabilitation of older structures. In this paper, the behavior of brick masonry wall reinforced with externally bonded of CFRP composites is studied with experimental and numerical investigations. The obtained experimental results have been validated by a new modeling technique based on the DMM approach. The following conclusions were drawn from the experimental and numerical study:

- the increase in the proportion of sand in the mortar (from 3 to 5) led to an increase in the shear strength and the ductility of the masonry panels, especially in the case of reinforcement.

- The improvement in shear strength for strengthened wall panels with CFRP composite ranged from 3 to 4 times (65% to 270%).
- All reinforced wall panels showed a substantial increase in the ductility by 73% to 88% compared with unreinforced wall panels.
- The most significant increase in ductility was achieved by reinforcement in both sides of the wall panel by X shape with talents (MRX).
- The Finite Element model proposed in this paper shows considerable accuracy for the prediction of maximum shear load and failure mode.
- The developed model has been proved to capture the crack patterns and the stress distribution patterns in both of the brick and mortar.
- The CDP model is an appropriate hypothesis to represent the damage and the non-linear behaviour of brick and mortar.
- The behavior of the masonry is strongly governed by the behavior of the interface, Coulomb friction criterion are important to simulate the load transmission correctly between brick and mortar.

The good correlation between experimental and numerical curves encourages us to use this model in further works for the study of all type of unreinforced or reinforced masonry structure.

In addition, several factors such as type of loading and the characteristics of the single component brick and mortar should be considered in future researches in order to develop a suitable and optimal design approach for strengthening of in-plane loaded masonry walls. The numerical results for strengthened masonry wall will be discussed in future work.

Acknowledgement

The authors gratefully thank the CNERIB laboratory of Algeria for their availability to carry out this work.

References

[1] Martinné Dörömbözi Piroska (2007): Reinforcing and rehabilitation of stone structures, Építőanyag-Journal of Silicate Based and Composite Materials 59, 77-81. http://dx.doi.org/10.14382/epitoanyag-jsbcm.2007.12

[2] O. Csicsely Ágnes (2011): Short presentation of life cycle of earth construction, Építőanyag Journal of Silicate Based and Composite Materials 3-4, 42-47. http://dx.doi.org/10.14382/epitoanyag-jsbcm.2011.7

[3] Mahmood, H. and Ingham, J. M. (2011) Diagonal Compression Testing of FRP-Retrofitted Unreinforced Clay, *Journal of Composites for Construction,* 15(5):810-820. DOI: 10.1061/(ASCE)CC.1943-5614.0000209

[4] Valluzzi, M. R. – Tinazzi, D. – Modena, C. (2002) Shear behavior of masonry panels strengthened by FRP laminates, *Construction and Building Materials*, vol. 16, no. 7, pp. 409–416. https://doi.org/10.1016/S0950-0618(02)00043-0

[5] Haroun, M. – Mosallam, A. – Allam, K. (2001): Cyclic In-Plane Shear of Concrete Masonry Walls Strengthened by FRP Laminates. In Proceedings of Seventh International Symposium on Fiber Reinforced Polymers for Reinforced Concrete Structures, vol. SP-230-19, 327-339. ACI, Kansas City.

[6] Tumialan, G. – Morbin, A. – Nanni, A. – Medena, C. (2001): Shear Strength of Masonry Walls with FRP Composites. In COMPOSITES 2001 convention and Trade Show, Composites Fabricators Association, 6.

[7] Hamid, A. – El-Dakhakhani, W. – Hakam, Z. – ElGawady, M. (2005): Behavior of Composite Unreinforced Masonry-Fiber-Reinforced Polymer Wall Assemblages Under In-Plane Loading. *Journal of Composites for Construction*, 9(1), 73-83. https://doi.org/10.1061/(ASCE)1090-0268(2005)9:1(73)

[8] Li, T. – Silva, P. – Belarbi, A. – Myers, J. (2001): Retrofit of Un-Reinforced Infill Masonry Walls with FRP." In Proceedings CCC 2001 Composites in Construction, Porto, Portugal, October 10-12, 2001.

[9] ElGawady, M. A. – Lestuzzi, P. – Badoux, M., (2005): In-Plane Seismic Response of URM Walls Upgraded with FRP, *Journal of Composites for Construction*,vol. 9, no. 6, pp. 524–535. https://doi.org/10.1061/(ASCE)1090-0268(2005)9:6(524)

[10] Dizhur, D. – Griffith, M. – J. Ingham, (2013): In-Plane Shear Improvement of Unreinforced Masonry Wall Panels Using NSM CFRP Strips, *Journal of Composites for Construction*, vol. 17, no. 6, https://doi.org/10.1061/(ASCE)CC.1943-5614.0000400

[11] Korany, Y. – Drysdale, R. (2006): Rehabilitation of Masonry Walls Using Unobtrusive FRP Techniques for Enhanced Out-of-Plane Seismic Resistance, *Journal of Composites for Construction*, vol. 10, no. 3, pp. 213–222. https://doi.org/10.1061/(ASCE)1090-0268(2006)10:3(213)

[12] Lourenco, P. B. (1996): *Computational Strategies for Masonry Structures*, PhD thesis, Delft University of Technology, Delft, The Netherlands.

[13] Lourenço, P. B. (2008): Structural masonry analysis: recent developments and prospects.In: proceding of the 14th International Brick and Block Masonry conference,Sydney, Australia

[14] D'Altri, A. M. – de Miranda S. – Castellazzi G. – Sarhosis V.(2018): A 3D detailed micro-model for the in-plane and out-of-plane numerical analysis of masonry panels. *Computers & Structures*, 206. pp. 18-30. https://doi.org/10.1016/j.compstruc.2018.06.007

[15] Cristian Sandoval – Oriol Arnau (2017): Experimental characterization and detailed micro-modeling of multiperforated clay brick masonry structural response. *Materials and Structures* 50(34) :1-17. https://doi.org/10.1617/s11527-016-0888-3

[16] EN 771-1, Specification for masonry units – Part 1: Clay masonry units. European Standard (2003).

[17] EN 1015-11, Methods of test for mortar for masonry. Determination of flexural and compressive strength of hardened mortar, European Standard (2007).

[18] RILEM. LUMB1(1994) Compressive strength of small walls and prisms. Technical Report, RILEM.

[19] ASTM (2002). ASTM E 519-02, Standard Test Method for Diagonal Tension (Shear) in Masonry Assemblages. ASTM International, West Conshohocken, PA

[20] Lubliner, J. – Oliver, J. – Oller, S. – Onate, E. (1989): A plastic-damage model for concrete. International Journal of Solids and Structures, 25;25(3):299-326. https://doi.org/10.1016/0020-7683(89)90050-4

[21] Dassault Systemes, Abaqus/CAE. USA (2014) Dassault Systemes Simulia Corp.

Ref.:
Hernoune, Houria – **Benabed**, Benchaa – **Alshugaa**, Madyan – **Abousnina**, Rajab – **Guettala**, Abdelhamid: *Strengthening of masonry walls with CFRP composite: experiments and numerical modeling*
Építőanyag – Journal of Silicate Based and Composite Materials, Vol. 72, No. 1 (2020), 2–11. p.
https://doi.org/10.14382/epitoanyag-jsbcm.2020.1

Evaluation of index and compaction properties of lateritic soils treated with quarry dust based geopolymer cement for subgrade purpose

Kennedy Chibuzor ONYELOWE ▪ Department of Civil Engineering, Michael Okpara University of Agriculture, Nigeria ▪ konyelowe@mouau.edu.ng
Duc BUI VAN ▪ Research Group of Geotechnical Engineering, Construction Materials and Sustainability, Hanoi University of Mining and Geology, Vietnam
Lam DAO-PHUC ▪ Research Group of Geotechnical Engineering, Construction Materials and Sustainability, Hanoi University of Mining and Geology, Vietnam
Favour ONYELOWE ▪ Department of Biotechnology, Faculty of Science, Ebonyi State University, Nigeria
Chidozie IKPA ▪ Department of Civil Engineering, Faculty of Engineering, Alex Ekwueme Federal University, Nigeria
Charles EZUGWU ▪ Department of Civil Engineering, Faculty of Engineering, Alex Ekwueme Federal University, Nigeria
A. Bunyamin SALAHUDEEN ▪ Department of Civil Engineering, Faculty of Engineering, University of Jos, Nigeria
Michael MADUABUCHI ▪ Department of Civil Engineering, Michael Okpara University of Agriculture, Nigeria
Jesuborn OBIMBA-WOGU ▪ Department of Civil Engineering, Michael Okpara University of Agriculture, Nigeria
Kizito IBE ▪ Department of Civil Engineering, Michael Okpara University of Agriculture, Nigeria
Light IHENNA ▪ Department of Civil Engineering, Michael Okpara University of Agriculture, Nigeria

Érkezett: 2019. 11. 29. ▪ Received: 29. 11. 2019. ▪ https://doi.org/10.14382/epitoanyag-jsbcm.2020.2

Abstract

The effect of quarry dust based geopolymer cement on the index and compaction characteristics of soft problematic soils has been studied in the laboratory. The particular interest was on the geopolymer cement treatment of test problematic soils subgrade as hydraulically bound materials. In pavement foundation constructions, particular emphasis is always placed on how moisture suction and capillary actions affect the performance of the subgrade layer. Lateritic soils, which form the compacted foundation of pavements have the tendency to behave like plastics or liquids when in contact with moisture. These factors affect substantially the behavior and overtime performance, which is the durability of pavement subgrades. The primary aim of this research work was to adapt geopolymer cement synthesized from valorized solid waste materials (quarry dust and metallurgical slag). Laboratory experiments were used in this study. The test soils were observed to belong to A-2-6, A-2-7 and A-7 soils according to AASHTO classification, which are highly plastic and expansive. They are also of high clay content, a property which makes them unsuitable as moisture bound materials in foundations. The quarry dust based geopolymer cement was utilized at the rate of 10 to 150% by weight of dry soil in an increment of 10%. The test soils treatment protocol shows that the additive consistently improved the plasticity index and maximum dry density of the treated soils obtained at optimum moisture condition. The results have shown that the environmentally friendly cement derived from the valorization of solid waste has improved the properties of the compacted earth utilized under moisture bound environment. So, it stands as a good replacement for ordinary cement.

Keywords: index properties, silicate-based materials, moisture bound composite materials, solid waste valorization, soil compaction, geopolymer cement, geotechnics
Kulcsszavak: szilikát alapú anyagok, szilárd hulladék felhasználása, talaj tömörítés, geopolimer cement, geotechnika

Kennedy Chibuzor ONYELOWE
is a senior lecturer and researcher at the department of civil engineering, Michael Okpara University of Agriculture, Umudike, Nigeria, an adjunct senior lecturer at the department of civil engineering, Alex Ekwueme Federal University, Ndufu Alike Ikwo, Abakaliki, Nigeria and the principal investigator of the Research Group of Geotechnical Engineering, Construction Materials and Sustainability, Hanoi University of Mining and Geology, Hanoi, Vietnam. His research areas include soil stabilization, computational geotechnics, environmental geotechnics, structural construction materials, solid waste recycling wastes based geomaterials and geotechnical engineering.

Duc BUI VAN
is a lecturer at the Hanoi University of Mining and Geology, Hanoi, Vietnam and member of the research group of Geotechnical engineering, Construction Materials and sustainability, HUMG, Vietnam. His research area is geotechnical engineering.

Lam DAO-PHUC
is a professor of Geotechnical engineering at the HUMG and another important member of the research group of Geotechnical engineering, Construction Materials and sustainability, HUMG, Hanoi, Vietnam. He is also a published researcher in this field.

Favour ONYELOWE
is an undergraduate student of the department of biotechnology, Ebonyi state university, Abakaliki, Nigeria. She is also a contributing author in the area of biomass and greenhouse emission sequestration during the combustion stage of ash derivation.

Chidozie IKPA
is currently a technologist in the department of civil engineering laboratory of the Alex Ekwueme University, Ndufu Alike Ikwo, Nigeria. His research areas are construction materials, pavement materials, highway engineering and geotechnical engineering.

Charles N. EZUGWU
is an Associate professor and the head of the department of civil engineering at the Alex Ekwueme Federal University Ndufu Alike Ikwo, Nigeria. His research areas are water and environmental engineering, materials engineering, waste recycling.

A. Bunyamin SALAHUDEEN
is senior lecturer and researcher at the University of Jos, Nigeria. His research areas are geotechnical engineering, construction materials, soil mechanics, computational geotechnics, etc. He is a member of many professional and learned societies.

1. Introduction

Index properties of soils are the consistency behavioral patterns soils exhibit within the liquid and plastic phases when they are mixed with moisture. The liquid and plastic behaviors of soft cohesive fine-grained soils determine the soils abilities to be molded, rolled or compacted under different molding moisture conditions [1]. Liquidity of soils is very important in soil mechanics and foundation engineering as it determines certain design factors more especially when the materials are under hydraulically bound conditions [2]. Similarly, the compactibility of soils depend also on the molding moisture conditions or the consistency under which the compaction is carried out [3]. Compaction is a mechanical process of soil stabilization but the state of the soil being compacted plays a

big role on the outcome of the compaction process [4]. For instance, highly plastic soils with plasticity index above 17%, are difficult to handle compared to medium, less or non-plastic soils [5]. It is important to note that both properties of consistency and compaction are the responses of soils when mixed with moisture [6]. They both are moisture limits within which soils characteristics are determined [7]. In compaction, the maximum density of soils is achieved at a moisture intake mark called the optimum moisture [8]. The whole aim is to achieve densification of soil mass in a pavement foundation procedure [8]. But in this case, an ecofriendly supplementary cementitious compound has been developed to enhance the index and compaction properties of soft soils utilized as pavement underlain in the laboratory [1-4]. Researchers are working hard in this line to develop composite geomaterials that replace the conventional methods or materials, which bring about greenhouse emissions [9]. And one of such materials is the quarry dust based geopolymer cement, which was utilized to treat soils in varying proportions [10]. This cementitious compound is a combination of quarry dust, metallurgical slag and alkali activators [11]. Both quarry dust and metallurgical slag are industrial waste materials from quarry and metal operations. Quarry dust and metallurgical slag have been in use as stabilization silicate-based agents in the improvement of the mechanical properties of soils especially problematic soils for use as pavement subgrade materials [11]. This has been successful because of the high content of aluminosilicates possessed by these waste materials from quarry and metal operations. Their pozzolanic properties as single independent admixtures have been incorporated into the composite silicate-based cement compound synthesized under the reactive influence of alkali activators [11-13]. This work studied the effect of quarry dust based geopolymer cement on the index and compaction characteristics of treated problematic soils to be utilized as pavement foundation materials.

2. Methodology

2.1 Materials preparation

Three different borrow pit locations, with coordinates 5°29'16" North and 7°28'58" East (Olokoro location), 5°27'0" North and 7°31'60" East (Amaba location), and 5°31'0" North and 7°26'0" East (Ohia location), were the source point of the test soils. Lumps were eliminated by tapping with rubber pestle, and open dried for four days to start of experiment procedure. Fundamental properties, particle size distribution and chemical compounds composition of the three studied soil specimens and test materials are presented in the *Table 1, Fig. 1* and *Table 2*. The test soils have high free swell indexes and low shrinkage limits. This desiccation behavior makes the soils unsuitable as foundation materials. Exposure of these untreated test soils to moisture for a long time creates room for failures of infrastructures constructed on these soils because of the high potential to swell. It is also observed that the soils are highly plastic. This property also makes the untreated material unsuitable to be utilized as subgrade materials or as hydraulically bound materials. The A-2-7, A-2-6 and A-7 test soils are observed to be poorly graded soils [14]. Soils A and C contain high percentage of clay and are designated as highly clay (CH) content soils, which is a property responsible for the expansivity of clayey soils in contact with moisture. *Table 2* presents that the test materials have high percentage of aluminosilicate compounds. Quarry dust (QD) also contains high pozzolanic property [11]. The quarry dust based Geopolymer cement was synthesized according to the procedures and findings of Davidovits [12-13]. The aluminosilicate materials required to materialize the Geopolymer cements consist of quarry dust. The geopolymer cements synthesis was activated by the reactive stimulus of Sodium Hydroxide (NaOH) and Sodium Silicate (Na_2SiO_3) [12-13]. According to previous research findings, a molarity concentration NaOH of 12 was used to achieve an environmentally friendly material handling and construction process and better strength properties of geopolymer cement might be attained. The synthesis of geopolymer matrixes was carried out by mixing these above materials in a proportion of 4.8% activator, plus 80% quarry dust by weight and 15% metallurgical slag by weight [12-13].

Property description of test soils and units	Values / Descriptions		
	Soil (A)	Soil (B)	Soil (C)
% Passing Sieve, No 200	2.85	10	4.6
NMC (%)	12.1	13.49	14
LL (%)	40	46	64
PL (%)	18	21	36
PI (%)	22	25	28
SL (%)	8	8	7
FSI (%)	250	250	275
G_s	2.6	2.43	2.12
AASHTO Classification	A-2-7	A-2-6	A-7
USCS	GP, CH	GP	GP, CH
MDD (g/cm³)	1.76	1.85	1.80
OMC (%)	13.1	16.2	13.13
CBR (%)	12	13	8
Color	Reddish Brown	Reddish Gray	Reddish Ash

Table 1 Basic properties of test soils
1. táblázat A vizsgált talajok alapvető tulajdonságai

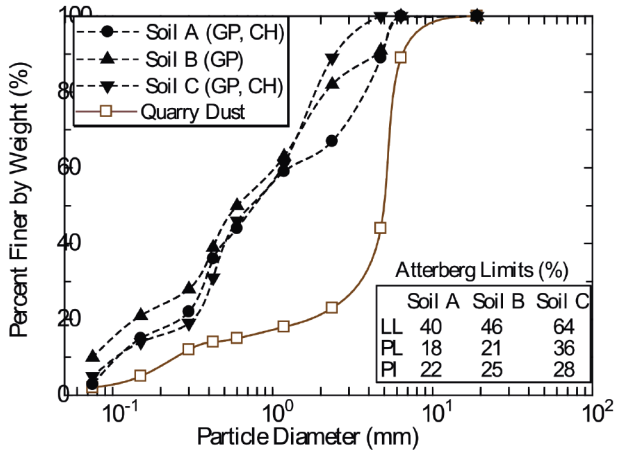

Fig. 1 Grain size distribution of studied materials
1. ábra A vizsgált anyagok szemmegoszlása

Materials	Oxides composition (content by wt %)												
	SiO_2	Al_2O_3	CaO	Fe_2O_3	MgO	K_2O	Na_2O	TiO_2	LOI	P_2O_5	SO_3	IR	Free CaO
Soil A	76.56	15.09	2.30	2.66	0.89	2.10	0.33	0.07	-	-	-	-	-
Soil B	77.57	14.99	3.11	1.78	0.86	1.45	0.23	0.01	-	-	-	-	-
Soil C	77.73	16.65	1.42	3.22	0.07	0.89	0.02	-	-	-	-	-	-
QD	63.48	17.72	5.56	1.77	4.65	2.76	0.01	3.17	0.88	-	-	-	-

**IR is Insoluble Residue, LOI is Loss on Ignition, QD: Quarry Dust*

Table 2 Chemical oxides compounds composition of the materials used in this paper
2. táblázat A viszgált anyagok kémiai összetétele

2.2 Experimental methods

Preliminary conventional tests; particle size distribution, Atterberg limits, compaction, free swell test and shrinkage limit tests, were conducted to determine the basic properties of the test soils in accordance with British standards [15-17].

Laboratory tests were conducted on the soils treated with varying proportions of quarry dust based geopolymer cement (QDbGPC) at the rate of 10%, 20%, 30% to 150% by weight of the dry soil to the determine the index properties of the treated soils in accordance with British Standards [16]. Similarly, the standard proctor compactive effort was used on test involving moisture/density relationship. Air dried soils samples passing through sieve number 4 (4.76 mm aperture BS sieve) mixed with 10%, 20%, 30% to 150% by weight of the dry soil of the ecofriendly binding admixture were used. The Standard Proctor procedure was conducted in the laboratory in accordance with British Standard [16].

3. Results and analysis

3.1 Consistency limits and compaction behavior

The consistency behavior of QDbGPC treated uncemented lateritic soils are presented in *Fig. 2.* The plasticity indexes (PI) of the natural untreated lateritic soils were recorded as 22, 25 and 28% respectively. These were considered highly plastic soils and undesirable as construction materials. Upon the treatment of these soils with QDbGPC, the PI was observed to reduce consistently at the rate of 18%, 8% and 4% respectively at 10% by weight utilization of the geopolymer cement. On further treatment with the geopolymer cement at 20% to 100% by weight utilization, the PI consistently reduced at the rate of 9% for treated soils A and B and 13% for treated soil C. At 130%, 140% and 150% utilization of the geopolymer cement, the consistency behavior of soil A showed a steady PI of 4%. This observed behavior of the treated soils has been contributed by increased calcium content from the geopolymer cement blend to hydration reaction and calcination. This was also due to the rearrangement of molecules during the formation of transitional compounds. The hydration and calcination of the treated soils under high proportional aluminosilicate and pozzolanic geopolymer cement had caused this improvement. This however, produced stabilized treated soils of stiff consistency. Moreover, the cations release deposited at the adsorbed complex interface of the treated soils from the synthesized geopolymer cement constituents during the cation exchange reaction had also caused this reaction [18-19]. This proves that the mechanical factors of the treated soils would remain steady with the usual reduction in the liquid limits on addition of the treatment material if water is used as pore fluid. With the foregoing, under the addition of varying proportions of quarry dust based geopolymer cement, it can be deduced that the liquid limits and plasticity indexes depend on the mechanical conditions rather than the viscosity of pore fluid and density of the treated matrix [18-20]. But to a higher degree, this treatment protocol results is a function of carbonation, cation exchange, polymerization and polycondensation, which are physicochemical properties. Having achieved treated materials matrix of plasticity index below 15%, the utilization of quarry dust based geopolymer cement has improved the treated lateritic soils such that they can best be used at non-frost-susceptible subgrade and subbase materials. That is to say that under hydraulically bound or moisture bound conditions, the materials can adjust with great flexibility to withstand the effect of that exposure. However, the goal of achieving a durable pavement or foundation facility would have been successful. Similarly, the results of the compaction behavior of the treated lateritic soils are presented in *Fig. 3*. The maximum dry density (MDD) improved consistently from 1.76, 1.85 and 1.80 g/cm^3 respectively at 0% by weight utilization of quarry dust based geopolymer cement to 2.125, 2.5, and 1.95 g/cm^3 respectively at 150% by weight utilization of quarry dust based geopolymer cement. On the other hand, the optimum moisture reduced in a consistent trend also. Moisture was required to cause a dissociation of cations and anions from the geopolymer cement during hydration to supply more Ca^{2+} for the cation exchange reaction [11]. This cation exchange reaction caused the consistent reduction of moisture content, which led to the formation of flocs of the clay particles hence the densification of the treated soils.

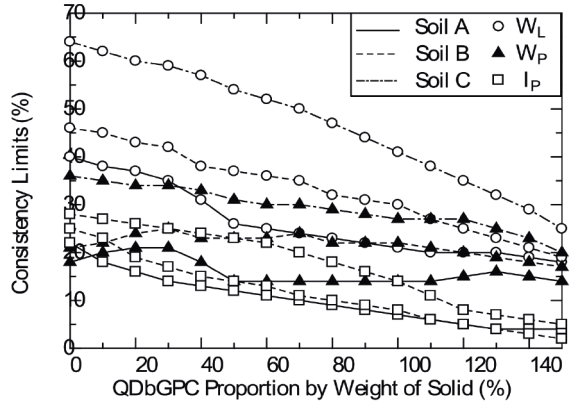

Fig. 2 Consistency limits of QDbGPC treated soils
2. ábra A QDbGPC-vel kezelt talajok tömörödési határértékei

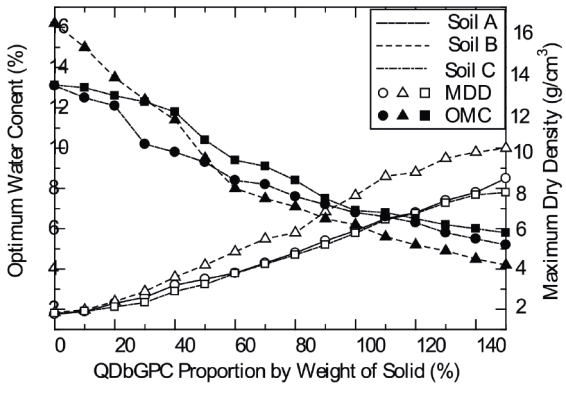

Fig. 3 Compaction behavior of QDbGPC treated soils
3. ábra A QDbGPC-vel kezelt talajok tömörödési viselkedése

4. Conclusions

The effect of solid waste based composite silicate based geopolymer cement, the quarry dust based geopolymer cement on the treated problematic soils has been observed under laboratory experiments. After the soils were treated through deep mixing with varying proportions of the composite ecofriendly cement, the index and compaction characteristics of the soils showed substantial and consistent improvement. The highly plastic soils improved to less plastic soils with plasticity indexes below 7% while the maximum dry densities obtainable at the optimum moisture condition also improved to good compactness. With the above observations, the quarry dust based composite geopolymer cement has proven to be a good supplementary cementing material for the stabilization of problematic soils and the improvement of the index and compaction properties when used as pavement subgrade materials exposed to moisture conditions.

Acknowledgement

The authors also would like to sincerely thank Vietnam Ministry of Education and Training for funding this research, Grant No. MOET /2019 with project number B2019-MDA-08.

References

[1] Onyelowe, K. C. – Bui Van, D.: Durability of nanostructured biomasses ash (NBA) stabilized expansive soils for pavement foundation, International Journal of Geotechnical Engineering, 2018. https://doi.org/10.1080/19386362.2017.1422909

[2] Onyelowe, K. C. – Bui Van, D.: Predicting Subgrade Stiffness of Nanostructured Palm Bunch Ash Stabilized Lateritic Soil for Transport Geotechnics Purposes. Journal of GeoEngineering of Taiwan Geotechnical Society, 2018. http://140.118.105.174/jge/index.php

[3] Onyelowe, K. C. – Bui Van, D.: Structural analysis of consolidation settlement behaviour of soil treated with alternative cementing materials for foundation purposes. Environmental Technology & Innovation, Vol. 11, 2018, pp. 125-141. https://doi.org/10.1016/j.eti.2018.05.005

[4] Onyelowe, K. C. – Bui Van, D.: Predicting Strength Behaviour of Stabilized Lateritic Soil- Ash Matrix using Regression Model for Hydraulically Bound Materials Purposes, International Journal of Pavement Research and Technology, 2018. https://doi.org/10.1016/j.ijprt.2018.08.004

[5] Onyelowe, K. C. – Bui Van, D. – Eberemu, A. O. – Xuan, M. N. – Salahudeen, A. B. – Ezugwu, C. – Van, M. N. – Orji, F. – Sosa, F. – Duc, T. T. – Amhadi, T. – Ikpa, C. – Ugorji, B.: Sorptivity, swelling, shrinkage, compression and durability of quarry dust treated soft soils for moisture bound pavement geotechnics. Journal of Materials Research and Technology, 8(4), 2019:3529–3538. https://doi.org/10.1016/j.jmrt.2019.06.029

[6] Tan, Y. – Hu, M. – Li, D.: Effect of agglomerate size on California bearing ratio of lime treated lateritic soils. International Journal of Sustainable Built Environment, Vol. 5 (1), 2016, Pp. 168-175. https://doi.org/10.1016/j.ijsbe.2016.03.002

[7] Onyelowe, K. C. – Bui Van, Duc – Ubachukwu, Obiekwe – Ezugwu, Charles – Salahudeen, Bunyamin – Nguyen Van, Manh – Ikeagwuani, Chijioke – Amhadi, Talal – Sosa, Felix – Wu, Wei – Ta Duc, Thinh – Eberemu, Adrian – Pham Duc, Tho – Barah, Obinna – Ikpa, Chidozie – Orji, Francis – Alaneme, George – Amanamba, Ezenwa – Ugwuanyi, Henry – Sai, Vishnu – Kadurumba, Chukwuma – Selvakumar, Subburaj – Ugorji, Benjamin: Recycling and Reuse of Solid Wastes; a Hub for Ecofriendly, Ecoefficient and Sustainable Soil, Concrete, Wastewater and Pavement Reengineering. International Journal of Low-Carbon Technologies. Vol. 14(3), 2019, pp. 440-451. https://doi.org/10.1093/Ijlct/Ctz028

[8] Onyelowe, K. C. – Salahudeen, A. B. – Eberemu, A. O. – Ezugwu, C. N. – Amhadi, T. – Alaneme, G.: Oxides of Carbon Entrapment for Environmental Friendly Geomaterials Ash Derivation. In book: Recent Thoughts in Geoenvironmental Engineering, Proceedings of the 3rd GeoMEast International Congress and Exhibition, Egypt 2019 on Sustainable Civil Infrastructures – The Official International Congress of the Soil-Structure Interaction Group in Egypt (SSIGE), 2020, pp. 58-67. https://doi.org/10.1007/978-3-030-34199-2_4

[9] K. C. Onyelowe, – A. B. Salahudeen, – A. O. Eberemu, – C. N. Ezugwu, – T. Amhadi, – G. Alaneme – F. Sosa: Utilization of Solid Waste Derivative Materials in Soft Soils Re-engineering. In book: Recent Thoughts in Geoenvironmental Engineering, Proceedings of the 3rd GeoMEast International Congress and Exhibition, Egypt 2019 on Sustainable Civil Infrastructures – The Official International Congress of the Soil-Structure Interaction Group in Egypt (SSIGE), 2020, pp. 49-57. https://doi.org/10.1007/978-3-030-34199-2_3

[10] Onyelowe, K. C. – Amhadi, T. – Ezugwu, C. N. – Onukwugha, E. – Ugwuanyi, H. – Jideoffor, I. – Ikpa, C. – Iro, U. – Ugorji, B.: Cemented Lateritic Soil as Base Material Improvement Using Compression. In book: Innovative Infrastructure Solutions using Geosynthetics, Proceedings of the 3rd GeoMEast International Congress and Exhibition, Egypt 2019 on Sustainable Civil Infrastructures – The Official International Congress of the Soil-Structure Interaction Group in Egypt (SSIGE), 2020, pp. 58-67. https://doi.org/10.1007/978-3-030-34242-5_4

[11] American Standard for Testing and Materials (ASTM) C618. Specification for Pozzolanas. ASTM International, Philadelphia, 1978, USA.

[12] Davidovits, J.: Geopolymer Cement a review. Institute Geopolymer, F-02100, 2013, Saint-Quentin, France. [online]

[13] Abdel-Gawwadm, H. A. – Abo-El-Enein, S. A.: A Novel Method to Produce Dry Polymer Cement Powder. HBRC Journal. Vol. 12, 2016 Pp. 13-24. http://dx.doi.org/10.1016/j.hbrcj.2014.06.0018

[14] American Administration for State Highway Officials., AASHTO. Guide for Design of Pavement Structures, AASHTO, 1993, California, USA

[15] BS 1377 - 2, 3. Methods of Testing Soils for Civil Engineering Purposes, British Standard Institute, 1990, London.

[16] BS 1924. Methods of Tests for Stabilized Soil, British Standard Institute, 1990, London.

[17] Nigerian General Specification. Specification for Construction of Roads and Bridges, 1997, Nigeria.

[18] American Administration of State Highway and Transportation Officials, AASHTO T 22-03. Standard Method of Test for Compressive Strength of Cylindrical Concrete Specimens, 2014, Washington DC.

[19] American Administration of State Highway and Transportation Officials, AASHTO T 193-81. Standard Method of Test for The California Bearing Ratio of Compacted Soils, 2013, Washington DC.

[20] Hamidi, R. M. – Man, Z. – Azizli, K. A.: Concentration of NaOH and the Effect on the Properties of Fly Ash Based Geopolymer. 4th International Conference of Process Engineering and Advanced Materials; Procedia Engineering, Vol. 148, 2016, Pp. 189-193. http://dx.doi.org/10.1016/j.proeng.2016.06.568

Ref.:
Onyelowe, Kennedy Chibuzor – **Bui Van**, Duc – **Dao-Phuc**, Lam – **Onyelowe**, Favour – **Ikpa**, Chidozie – **Ezugwu**, Charles – **Salahudeen**, A. Bunyamin – **Maduabuchi**, Michael – **Obimba-Wogu**, Jesuborn – **Ibe**, Kizito – **Ihenna**, Light: *Evaluation of index and compaction properties of lateritic soils treated with quarry dust based geopolymer cement for subgrade purpose*
Építőanyag – Journal of Silicate Based and Composite Materials, Vol. 72, No. 1 (2020), 12–15. p.
https://doi.org/10.14382/epitoanyag-jsbcm.2020.2

Studying compression strength of XD3 concrete samples after addition of calcium nitrate inhibitor and superplasticizers

Shaymaa Abbas ABDULSADA
PhD student in Faculty of Materials Science and Engineering, University of Miskolc, Hungary. Lecturer at Faculty of Engineering, University of Kufa, Iraq. Research Interests: Corrosion Engineering, Metallurgy Engineering, Heat Treatment of Metals, Casting of Metals.

Tamás I. TÖRÖK
Professor of Chemical Metallurgy and Surface Technologies at University of Miskolc, Hungary. First Secretary of HUNKOR, the Hungarian Corrosion Society, and former President of ASM International Hungary Chapter. Recent Research Interests: Corrosion Phenomena, Protective Coatings, Metals Surface Treatments and Surface Engineering.

Shaymaa Abbas ABDULSADA ▪ Faculty of Materials Science and Engineering, University of Miskolc, Hungary ▪ qkosha86@uni-miskolc.hu
Tamás I. TÖRÖK ▪ Faculty of Materials Science and Engineering, University of Miskolc, Hungary

Érkezett: 2019. 10. 08. ▪ Received: 08. 10. 2019. ▪ https://doi.org/10.14382/epitoanyag-jsbcm.2020.3

Abstract
This research paper presents an analysis of the compression strength properties of concrete samples in the function of their calcium nitrate inhibitor content. This low cost inorganic inhibitor was added to the concrete mix in concentrations of 1% and 3% by weight of cement in addition of two different superplasticizers (MapeiDynamon SR 31 and Oxydtron). The compressive strengths of the so prepared samples were checked according to the relevant European standard and were within the acceptable limits, so this inhibitor does not weaken this important property of the concrete samples. Moreover, the MapeiDynamon SR 31 superplasticizer even showed higher (acceptable) values compared to the other type of superplasticizer due to the difference between their ability in reducing the ratio of water of the concrete samples.
Keywords: calcium nitrate inhibitor, compression strength, superplasticizers, concrete samples
Kulcsszavak: kalcium-nitrát uinhibitor, nyomószilárdság, plasztifikáló adalékok, beton minták

1. Introduction

Corrosion of steel rebar in reinforced concrete structures is a serious problem which might cause significant human and economic losses. One of the most important reasons of corrosion in reinforced concrete is chloride attack. The main sources of chlorides are seawater and de-icing salts. Also, there are other sources of chlorides for example from gravels, sand, cement, water (being used for preparing the mixture of fresh concrete) and sometimes from (contaminated) steel rebar. In the subsistence of chloride, the protective passive stratum of steel is locally destroyed and the unprotected steel areas start dissolve. The formation of corroding products (rust) involves a substantial volume increase, i.e. the volume of corrosion products is greater than that of original steel bar. Therefore expansive stresses are induced around corroded steel bars causing possible cracking, spalling of concrete cover and loss of bond between steel and concrete, thus reducing the serviceability of concrete structures [1-9].

There are several methods used to minimize corrosion of steel in concrete, one of these is to use inhibitors. Among the available methods, the uses of corrosion inhibitors are cost-effective and easy to handle. Inhibitors are added to fresh concrete while migrating inhibitors are usually proposed for concrete repair. Inhibitors, such as zinc oxide, molybdates and borates, carboxylate ions, quaternary ammonium salts, and other organic compounds were studied [10].

The hardening process of concrete is one of the important factors which effects on the compressive strength of concrete. The binder in concrete is cement. The cement matrix is formed during the hydration process and binds the aggregates together. The basic elements in the production of Portland cement are limestone ($CaCO_3$), silica (SiO_2), alumina (Al_2O_3), iron oxide (Fe_2O_3) and other substances in minor quantities. To produce cement clinker, the raw materials are mixed, ground and burned in a rotary kiln at about 1450°C. The constituents react to form new minerals. The four major minerals in cement clinker are tricalcium silicate (C_3S), dicalcium silicate (C_2S), tricalcium aluminate (C_3A) and tetracalcium aluminoferrite (C_4AF). The minerals in the clinker begin to react when water is added. This series of chemical reactions is called the hydration process, and consists of various phases. It starts immediately, and the dominant reactions occur on the first day [11, 12]. However, the chemical reactions continue for months, or even years, slowing down gradually. In engineering practice, the hydration process is often supposed to be 'finished' after around 28 days when the representative strength is reached. It is presented schematically in *Fig. 1* according to Locher [13].

In cement hydration process, there are some amounts of calcium hydroxide (CH) remaining in the cement structure. Those remaining CH can be replaced by consuming them with silica to form additional calcium silicate hydrates (C-S-H) which is the main contribution of cement strength [14, 15]. This silicon dioxide (silica) can be found through the pozzolanic material known as pozzolan.

Superplasticizers are preferred in concrete preparation for their ability to reduce the water requirement while maintaining workability and enable the improvement of strength. *Fig. 2* illustrates the working mechanism of superplasticizer. Cement particles are dispersed by repulsive force generated by negatively charged superplasticizers (*Fig. 2/b*) as, for example, in our case by a modified acrylic polymer Mapei Dynamon SR 31, and the entrapped water would be released. Therefore, the flow characteristics of concrete are improved [16].

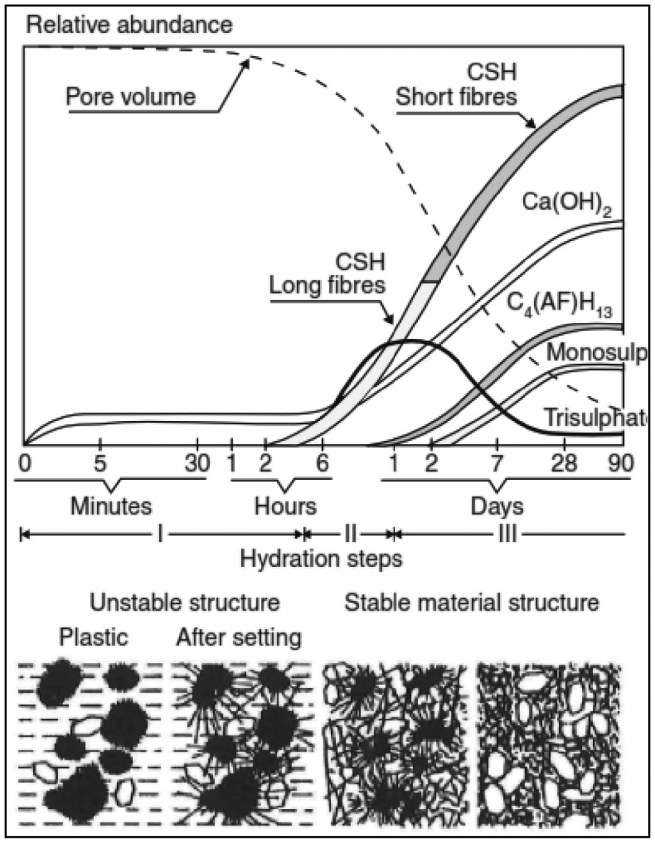

Fig. 1 Scheme of the hydration process according to Locher [13]. (Top) The development of the individual components and (bottom) schematic sketches of the material structure at 4 corresponding stages in time
1. ábra Hidraulikus kötés folyamata Locher szerint [13] Az egyes összetevők (fázisok) kialakulása (felül), és a megszilárduló anyag szerkezetének változása vázlatosan az időben (alul)

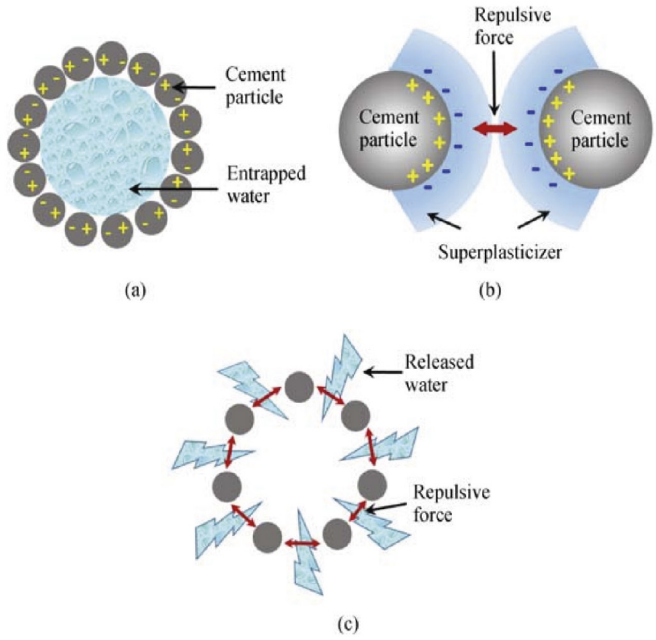

Fig. 2 Action of superplasticizer on cement particles. (a) Flocculated cement particles; (b) dispersing cement particles by the repulsive force generated by negatively charged superplasticizer; (c) releasing of entrapped water [16]
2. ábra Plasztifikáló adalék hatása a klinker ásványszemekre. (a) Flokkulálódott részecskék; (b) Cement/klinker részecskék diszpergálódása a negatív felületi töltésű plasztifikáló adalék hatására; (c) A fizikailag megkötődött víz felszabadulása [16]

The main purpose of this paper is to present the results of an experimental study on the compressive strengths to monitor and evaluate the effect of calcium nitrate inhibitor and superplasticizers of test samples prepared from concrete type XD3.

2.Materials and methods

2.1 Materials and preparation of samples

Portland slag cement CEM II/A-S 42.5R was used in this study conforming to the standard EN 197-1 [17] and it was received from CRH Magyarország Kft. company in Miskolc, Hungary. Aggregates (fine and coarse) were used according standard EN 12620 [18] and it was also received from the CRH Magyarország Kft. company. This type of cement chosen because it is very workable, has a progressive increase in its initial strength, has very good cement density and its resistance to chemical reactions is high. Calcium nitrate as a inorganic inhibitor and two types of superplasticizers (Mapei Dynamon SR 31 and Oxydtron) were used. Tap water was used for both making and curing the specimens.

Concrete mixes were designed in accordance with the European mix design method (XD3 class) to have compressive strength C35/45 at age of 28 days. Two times three samples were prepared (with the two different plasticizers) and the two sets of three plus three samples contained in 0%, 1%, 3% the calcium nitrate inhibitor as shown in *Table 1*. The concrete cubes so prepared for compressive strength testing had dimensions of 70×70 mm. The molds were thoroughly cleaned and oiled before casting to avoid adhesion with the concrete surface. Mixing of materials was done manually after that water added to the mix with continued mixing, then the mix was put in the molds.

The specimens were taken out from the molds after 24 hours hardening, then were immersed in tap water for 28 day as shown in *Fig. 3*.

Type of Mixtures		
Symbol of Mix	Type of Admixture	Concentration of Calcium Nitrate Inhibitor
A3 (Reference)	Mapei Dynamon SR 31	without
B3	Mapei Dynamon SR 31	1% by weight of cement
C3	Mapei Dynamon SR 31	3% by weight of cement
A4 (Reference)	Oxydtron	without
B4	Oxydtron	1% by weight of cement
C4	Oxydtron	3% by weight of cement

Table 1 The concrete mixtures (specimens) prepared for this study
1. táblázat Betonminták összetétele a jelen vizsgálatokhoz

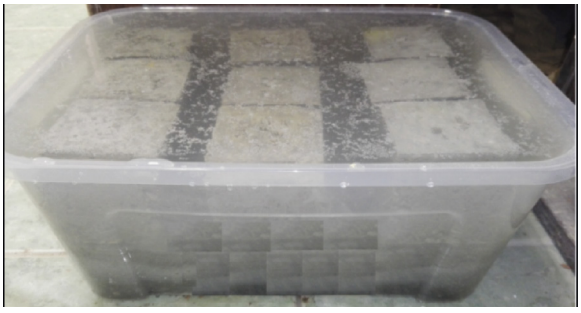

Fig. 3 Curing of compressive strength specimens in tap water
3. ábra Nyomószilárdság mérésére előkészített próbák érlelése csapvízben

2.2 Compressive strength test

The concrete compressive strength was measured by using a compressive strength testing machine (Kispesti Vas és Fém KTSZ) as shown in *Fig. 4*. The cubes were removed from the curing water at age of 28 days after that tested by compressive strength machine as shown in *Fig. 5*. The reported values are the average of three specimens for each age (nine for each mix).

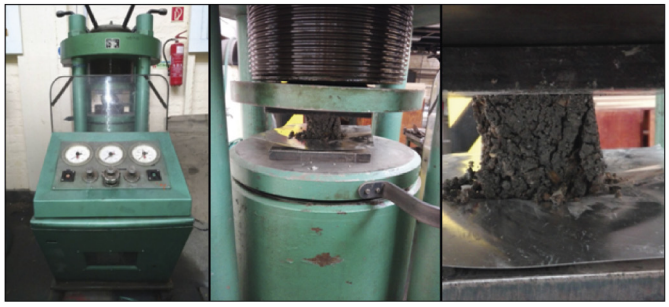

Fig. 4 Machine of compressive strength while sample testing
4. ábra Berendezés a nyomószilárdság mérésére

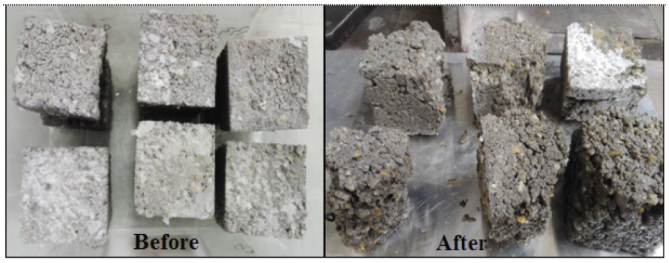

Fig. 5 Specimens before and after compressive strength testing
5. ábra Betonminták a nyomószilárdság mérése előtt és után

3. Results and disscusion

After adding calcium nitrate as a corrosion inhibitor, the results of compressive strength measurements was presented in *Fig. 6* and *Table 2*.

Symbol of Mix	Compressive Strength in MPa at 28 day
A3 - Reference (for comparing)	38
B3	41
C3	46
A4 - Reference (for comparing)	30
B4	32
C4	38

Table 2 Results of compressive strength test for samples with calcium nitrate inhibitor
2. táblázat Kalcium-nitrát inhibítort is tartalmazó teszt minták nyomószilárdság értékei

As it is illustrated in *Fig. 6* the samples without inhibitor has significantly lower compressive strength. In the samples with Dynamon SR 31 there was not much reduction observed in the compressive strength (about 38 MPa as average for 3 samples tested at age 28 days). While the samples with Oxydtron caused a greater decrease in compressive strength (about 30 MPa as average for 3 samples tested at age 28 days) than Dynamon SR 31 admixture.

(Without this admixtures (Dynamon SR 31 and Oxydtron) the given type of concrete should have a compression strength of C35/45 MPa at age 28 days.).

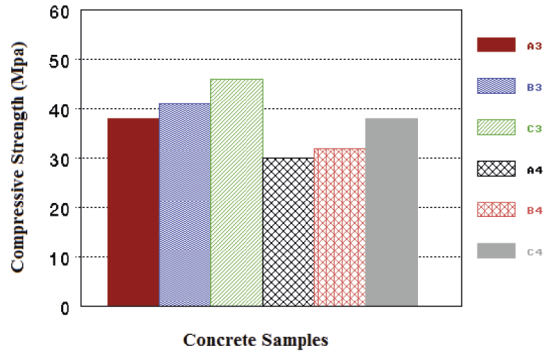

Fig. 6 Compressive strength of concrete samples with calcium nitrate inhibitor after immersion in tap water for 28 days
6. ábra Kalcium-nitrán inhibitort is tartalmazó betonminták nyomószilárdság értékei 28 napig csapvízben érlelés után

Comparing the effect of superplastisizers we found that Dynamon SR 31 caused reduction in water during the hardening process of concrete more than Oxydtron and this reduction in water caused increase in compressive strength of concrete and also decreased the porosity as a consequence of a series of chemical reactions (called hydration) of cement with water to form the binding material. The major compounds of cement (tricalcium silicate (C_3S), dicalcium silicate (C_2S), tricalcium aluminate (C_3A) and tetracalcium aluminoferrite (C_4AF)) begin to react with water within a few minutes and absorb the water then do not generate much strength, but can stiffen the mix and reduce workability, so if there's high quantity of water in the concrete that means the hydration components will be larger and these will decrease the capillary porosity and finally cause decrease in strength of concrete because the compressive strength depends also on the capillary porosity. So Dynamon SR 31 superplasticizer in this case more advantageous than Oxydtron superplasticizer.

By using calcium nitrate as corrosion inhibitor in conc. 1% and 3% by weight of cement and Dynamon SR 31 superplasticizer, the compressive strength increased considerably by 8% for 1% addition and 21% for 3% addition, respectively. While after using calcium nitrate inhibitor with 1% and 3% by weight of cement and Oxydtron superplasticizer, the compressive strength effected with an increase 7% for 1% addition and 27% for 3% addition, respectively.

The increase in compressive strength after adding calcium nitrate was due to that this admixture can accelerate the setting time and/or foster the development of higher early strength (calcium nitrate is a multifunctional admixture for concrete, i.e. it can work as setting accelerator for hydration process and as corrosion inhibitor). Calcium nitrate accelerates the hydration process because it has the same Ca^{2+} ion like the cement clinker minerals C_3S and C_2S. And, in presence of the water soluble calcium nitrate additive the crystallization processes can progress more intensively. The observed higher compressive strength with 3% calcium nitrate additive compared to the case with 1% can be attributed to the different compositions of the amorphous calcium silicate hydrate binders (CSH-gels) that will precipitate around the cement grains. An increased calcium

concentration in the pore water when calcium nitrate is also present may stabilize the CSH-gel causing a higher Ca/Si molar ratio and thus leading to the formation of polysilicate anions with shorter average length. The replacement of cement by calcium nitrate on the other hand, will lead to a CSH-gel with a lower Ca/Si ratio and longer length of the polysilicate anions, in addition to the formation of more gel due to the pozzolanic reaction [19-22]. Another contributing factor may be a change in morphology of calcium hydroxide due to a lower solubility caused by a higher Ca^{2+} concentration in the pore water, which agrees with several of researchers [23].

4. Conclusion

After testing the XD3 concrete samples with or without calcium nitrate inhibitors and two types of plasticizers we can conclude the following points:

- The compressive strength without calcium nitrate was higher in samples with Dynamon SR31(A3) than samples with Oxydtron (A4)
- The samples B3 and B4 (with 1% inhibitor) showed increase in compressive strength about 8% and 7% respectively.
- The compressive strength of the sample C3 (with 3% calcium nitrate inhibitor + Dynamon SR 31superplasticizer) was increased by 21%.
- The sample C4 (with 3% calcium nitrate inhibitor + Oxydtron superplasticizer) was the one that increased the most in the compressive strength after the addition of the inhibitor, where the increase was about 27%.

Acknowledgement

We would like to thank everyone who helped us to complete this research especially the efforts of the Institute of Metallurgy and Institute of Ceramic and Polymer Engineering, University of Miskolc in providing all the possibilities available to us in order to make the research successful.

References

[1] Abdulsada, S. A. – Fazakas, É. – Tamás, I. T. (2019): Corrosion testing on steel reinforced XD3 concrete samples prepared with a green inhibitor and two different superplasticizers, Materials and Corrosion, Vol.70, No.7, pp.1262-1272. https://doi.org/10.1002/maco.201810695

[2] Abdulsada, S. A. – Tamás, I. T. – Fazakas, É., (2018): Preliminary Corrosion Testing of Steel Rebar Samples in 3.5%NaCl Solution with and without a Green Inhibitor, Építőanyag-Journal of Silicate Based and Composite Materials, Vol.70, No.2, pp.48-53. https://doi.org/10.14382/epitoanyag-jsbcm.2018.10

[3] Abdulsada, S. A. – Fazakas, É. – Török, T. I. (2018) Corrosion studies of steel rebar samples in neutral sodium chloride solution also in presence of a bio-based (green) inhibitor, International Journal of Corrosion and Scale Inhibition, Vol.7, No.1, pp.38-47. http://dx.doi.org/10.17675/2305-6894-2018-7-1-4

[4] Quraishi, M.A. – Nayak, D.K. – Kumar, R. – Kumar, V. (2017): Corrosion of Reinforced Steel in Concrete and Its Control: An overview, Journal of Steel Structures & Construction, Vol.3, No.1, pp.1-6. https://doi:10.4172/2472-0437.1000124

[5] Abdulsada, S. A. – Ali I. A. – Ali A.A. (2017): Studying the Effect of Eco-addition Inhibitors on Corrosion Resistance of Reinforced Concrete, Bioprocess Engineering, Vol.1, No.3, pp.81-86. http://doi: 10.11648/j.be.20170103.14

[6] Abosrra, L. – Ashour, A.F. – Youseffi, M. (2011): Corrosion of Steel Reinforcement in Concrete of Different Compressive Strengths, Journal of Construction and Building Materials, Vol. 25, No.10, pp.3915–3925. https://doi.org/10.1016/j.conbuildmat.2011.04.023

[7] Bertolini, L. – Elsener, B. – Pedeferri, P. – Redaelli, E. – Polder, R.B. (2014): Corrosion of Steel in Concrete: Prevention, Diagnosis, Repair, 2nd Edition, Wiley, New York.

[8] Broomfield, J. P. (2007): Corrosion of Steel in Concrete: Understanding, Investigation and Repair, Second Edition, CRC Press, Taylor & Francis, London.

[9] Hannant, D. J. (2000): Cement-based Composites, Chapter four in Comprehensive Composite Materials, Vol.4, pp.323-362. https://doi.org/10.1016/B0-08-042993-9/00098-X

[10] Sami, M. (2013): The Influence of Added Inhibitors on Corrosion of Steel in Concrete Exposed to Chloride Containing Solutions, Advances in Materials Science, Vol.13, No.2, pp.5-11. https://doi.org/10.2478/adms-2013-0004

[11] Jaap, W. (2013): Understanding the tensile properties of concrete, Woodhead Publishing Series in Civil and Structural Engineering: Number 48, Woodhead Publishing Limited.

[12] Preece, S.J. – Billinghamand, J. – King, A.C. (2000): On the initial stages of cement hydration, School of Mathematics and Statistics, University of Birmingham, Edgbaston, Birmingham B152TT. https://www.maths.nottingham.ac.uk/plp/pmzjb1/cem.pdf

[13] Locher, F.W. – Richartz, W. – Sprung, S. (1976): Setting of Cement–Part I: Reaction and Development of Structure, Zement-Kalk-Gips INTERN , Vol.29, No.10., pp.435 – 442.

[14] Mohamed, N. S., Ideris, N.I.A., Linda S.N.T., et al. (2018) Microstructural characterization of catalysis product of nanocement based materials: A review, E3S Web of Conferences, Vol.34, 01039. https://doi.org/10.1051/e3sconf/20183401039

[15] Saad, S.A. – Muhd, F.N. – Nasir, S. – Maisarah, A. (2015): Pozzolanic Reaction Mechanism of Rice Husk Ash in Concrete – A Review, Applied Mechanics and Materials, Vols. 773-774, pp.1143-1147. https://doi.org/10.4028/www.scientific.net/AMM.773-774.1143

[16] Guowei, M.A. – WANG, L. (2018): A critical review of preparation design and workability measurement of concrete material for large scale 3D printing, Frontiers of Structural and Civil Engineering, Vol.12, No.3, pp.382-400. https://doi.org/10.1007/s11709-017-0430-x

[17] EN 197-1 2000 Cement-Part 1: Composition, specifications and conformity criteria for common cements European Standard was Approved by CEN National Members

[18] EN 12620 2002 Aggregates for Concrete European Standard was Approved by CEN National Members

[19] Kičaitė, A. – Pundienė, I. – Skripkiūnas, G. (2017): The influence of calcium nitrate on setting and hardening rate of Portland cement concrete at different temperatures, IOP Conf. Series: Materials Science and Engineering, Vol.251, conference1. https://doi.org/10.1088/1757-899X/251/1/012017

[20] Karagöl, F. – Demirboğa, R. – Kaygusuz, M.A. – Yadollahi, M. M. – Polat, R. (2013): The influence of calcium nitrate as antifreeze admixture on the compressive strength of concrete exposed to low temperatures, Cold Regions Science and Technology, Vol.89, pp.30-35. https://doi.org/10.1016/j.coldregions.2013.02.001

[21] Popovics, S. (1992): Concrete materials, properties, specifications and testing, 2nd edition, William Andrew Publishing Noyes.

[22] Ramachandran, V. S. (1995): Concrete Admixtures Handbook, 2nd edition, Publishing Noyes.

[23] Justnes, H. – Nygaard, E. C. (1994): The Influence of Technical Calcium Nitrate Additions on the Chloride Binding Capacity of Cement and the Rate of Chloride Induced Corrosion of Steel Embedded in Mortars, International conference, Corrosion and corrosion protection of steel in concrete; 1994; Sheffield, Sheffield Academic Press, pp.491-502. https://www.tib.eu/en/search/id/BLCP%3ACN004860901/The-Influence-of-Technical-Calcium-Nitrate-Additions/

Ref.:
Abdulsada, Shaymaa Abbas – **Török**, Tamás I.: *Studying compression strength of XD3 concrete samples after addition of calcium nitrate inhibitor and superplasticizers*
Építőanyag – Journal of Silicate Based and Composite Materials, Vol. 72, No. 1 (2020), 16–19. p.
https://doi.org/10.14382/epitoanyag-jsbcm.2020.3

Material removal characteristics of Al-SiO_2 composite in WEDM

Subramaniam KUMARAVEL ▪ Department of Mechanical Engineering, Pondicherry Engineering College, India ▪ profkumaravel@gmail.com

Natarajan ALAGUMURTHI ▪ Department of Mechanical Engineering, Pondicherry Engineering College, India

Érkezett: 2019. 10. 20. ▪ Received: 20. 10. 2019. ▪ https://doi.org/10.14382/epitoanyag-jsbcm.2020.4

Abstract

Demand for particle reinforced composite materials gradually increases and that leads to the use of inexpensive particles or solid waste particles as a reinforcement phase to lower the cost of the composite. Silica sand (SiO_2) is an industrial waste that contributes to the strength of the aluminium matrix. Therefore, an attempt is made to use 10 wt. % of silicon dioxide as hardening of particles to obtain composite materials with an aluminium matrix. A stir casting method was used to produce the aluminium matrix. The mechanical and optical microstructural properties of the newly developed Al /SiO_2 composites were studied. Al / SiO_2 composites were processed using wire electrical discharge machining (WEDM) to optimize processing parameters such as pulse-on time (μs), pulse-off time (μs) and current (A) to improve material removal rate (MRR). The model was confirmed and good agreement was reached.

Keywords: composite, reinforcement, aluminium, matrix, parameters, current, model, microstructural

Kulcsszavak: kompozit, megerősítés, alumínium, mátrix, paraméterek, áram, modell, mikroszerkezet

Subramaniam KUMARAVEL

Department of Mechanical Engineering, Pondicherry Engineering College, Pondicherry is a Research Scholar. He did his UG at Madras University and PG (Engineering Design) at Anna University. He has published more than 20 research papers in reputed journals and conference proceedings He has published 4 books for both the civil and mechanical Engineering students. He has 15 years of teaching experience in Engineering colleges as well as in Universities.

Natarajan ALAGUMURTHI

Professor, Department of Mechanical Engineering, Pondicherry Engineering College, Pondicherry is an erudite and renowned academic scholar, a high profile scientist researcher, an able administrator, a great visionary and a socially conscious innovator. He did his Bachelor's degree in Mechanical Engineering at Government College of Engineering, Salem, Master degree in Energy Technology at the Pondicherry Engineering College, Pondicherry. He won the Pondicherry University Medal in recognition of the Outstanding Performance in the M.Tech (Energy Technology). He obtained the Best Project award for his M.Tech Project work titled, "Energy Conservation Study at Chengalvarayan Cooperative Sugar Mills Ltd, Periyasevalai, Tamilnadu". He received his Ph.D from Pondicherry University in recognizing his significant contribution in the area of Thermal aspects in Manufacturing. He has also made remarkable achievement in the areas of teaching, research, invention and extension activities. Starting from a modest career as a Lecturer in a Self-financing College, he rose to the present position of Professor at Pondicherry Engineering College, a premier technical institution. He had guided many dissertations and research projects in Mechanical Engineering and Energy Technology and has 250 Papers to his credit in reputed journals and various conference proceedings. He has teaching and research experience of 30 years out of which 10 years as professor and visited Singapore, Malaysia, UAE and Bangladesh.

1. Introduction

Composite materials, which are usually reinforced with microstructured particles in metal matrices, have the ability to obtain the properties of individual materials. Metal matrix composites (MMC) make it easier for companies involved in the processing of raw materials and the production of goods in factories to meet current and future requirements.Currently, the devotion of time and attention to acquiring knowledge on aluminium (Al) on every side of the planet are largely found owing to the fact that its distinctive property of inferior density, hostility to corrosion and exceptionally good mechanical properties [1]. The manufacturing of part or element from aluminum MMCs make them appealing for many structural component where lofty inflexibility, elevated strength and inferior weight are essential. Aluminum is suited to the weight loss applications [2]. In recent times, the aluminum MMCs have attracted throughout the world attention in virtue of their potentiality to replace massive equivalent, mostly in the automotive and energy area. Toughning of aluminum composite by spreading over the area with exquisitely divided ceramic particles has been evolved for the making of materials with superior stiffness for manufacturing industry. Aluminum MMCs were investigated, and it was established that the hardness of composite materials rises with the inclusion of strengthening reinforcements, and superior hardness is by virtue of the existence of tough ceramic matters in the composite [3].

Silica sand is marked as one of the most economical and hard ceramics particles of unambitious density, obtainable in huge amount as a secondary product of solid waste matter in the mass production of a glass factory [4]. The disposal of silica sand powder in a glass factory causes significant economic and environmental problems. The use of quartz sand strengthens the aluminum matrix and offers the advantages of processing industrial waste and reducing processing problems in a glass factory [5]. Therefore, compounds with quartz sand as a reinforcing substance will undoubtedly be beneficial for widespread use in the automotive and aerospace industries. This resarch concentrate on the utilization of unused industrial waste and dispersing it in an aluminum matrix to produce composite by stir casting process [6].The dissertate for this study is the efficient use of quartz sand, which is one of the residual manufacturing products generated in the glass plant, which argument significant economical and environmental problems. The need for high strength composites enhanced by ceramics particles is also gradually rising. Therefore, more efforts are being made to use silica sand waste being dumped in plants as a reinforcement particles to lower the price of the cost of the composite materials.

In the present work, the lack of hardness of pure Aluminum is amplified by incorporating 10 wt. % SiO_2. Wire EDM Process (WEDM) is a potential process that is useful for processing hard-to-manage materials [7]. WEDM is used to process advanced materials with a metal matrix (MMC) and conductive ceramics. Efforts were made to treat freshly prepared Al composite with 10 wt. % SiO_2 back up to hold superior material removal rate (MRR). Measured WEDM coefficients, such as pulse time (μs), pulse turn-off time (μs), and current (A), have been optimized to refine the MRR. Analysis of variance (ANOVA) was put to use as a means of finding the major noteworthy measurable factors in WEDM operation . Taguchi's L9 orthogonal matrices were over-decorated to estimate the net parameter space in just a few experiments.

2. Materials and manufacturing

Pure commercially available Aluminum is taken as a matrix, and 10% via weight of silica is taken as reinforcement. The properties of SiO_2 are proven in *Table 1*. The common particle size of SiO_2 used on this work was 50 μm.Although many production generation had been used for the producing of mining and metallurgical composites, stir casting technology were one of the dominant technology used within the industry. This method is commonly used to produce complex types of materials for the manufacturing industry.

Chemical Properties	
Crystal name	Monoclinic
Mineral name	Moganite
Chemical Formula	SiO_2
Mesh size	230
Size	53 μm
Thermal Properties	
Melting point	1760°C
Boiling Point°C	2240°C
Physical Properties	
Density g/cm³	2.33
Molar mass	59.96 g/mol

Table 1 Properties of silica sand
1. táblázat Kvarchomok tulajdonságai

In addition, the constant propagation of reinforcement in the matrix is very feasible due to constant agitation by the mixer.In this study, to achieve all of these benefits, a method of stir casting method was selected for the manufacture of MMC [8,9]. The required amounts of silica are stored together with a graphite crucible, motor and stirrer. Al-SiO_2 compounds were synthesized using a stirrer.

Pure Aluminum is melted in a coal furnace. A vortex was created at a temperature of 770 °C and then preheated quartz sand was gradually added to the molten metal and then thoroughly mixed with a stirrer for 20 minutes [10]. Uniform dispersion of the reinforcement in the matrix is achieved using a stirrer [11]. The drive speed was 550 rpm. *Fig. 1* shows die casting of a matrix consisting of Aluminum-SiO_2.

Fig. 1 The casting of Al/SiO_2
1. ábra Al/SiO_2 rudak

3. Results and discussion

Since the cutting operation can change the microstructure of the sample due to heating, cutting was done using a low-velocity diamond plate [12]. After assembly, grinding was performed to reduce surface damage caused by cutting discs. The grinding speed was maintained at about 150 rpm and was performed with increasing paper fineness of 240, 400, 600 and 1000. Small scratches caused by the final grinding operation are removed by polishing using powder flakes. *Fig. 2* shows a uniform distribution of reinforcement throughout the matrix. The particle content is smaller since the area is smaller. With a greater growth in the quantity of composite particles, the grain obstacles are visible.Reinforcing particles are dark in colour. The distribution of quartz sand is seen evenly in the Aluminum matrix. This is achieved by vigorous stirring with a stirrer. There are no pores around the quartz sand particles. Besides, there is no matrix region without reinforcement. It has also been found that there is a good interfacial compound in addition to a uniform distribution. The tensile strength (*Fig. 3*) of 0% by mass of Al is 7 MPa, and this value increases to 20 MPa for Al / SiO_2 with the addition of 5% by mass of SiO_2, which shows an improvement of 185% compared to pure Al. Similarly, for 10 wt. % SiO_2, the tensile strength will increase to 29 MPa, that is approximately 315% better than the tensile power of unreinforced Aluminum. This is because the reinforcing particles in the compounds of the metal matrix are evenly distributed. But adding more reinforcing particles leads to agglomeration, which reduces the bond strength between Al and the reinforcing particles. An increase in SiO_2 will lead to greater cracking and consequently to lower tensile strength. Besides, contacts between silica particles will isolate ductile Aluminum.

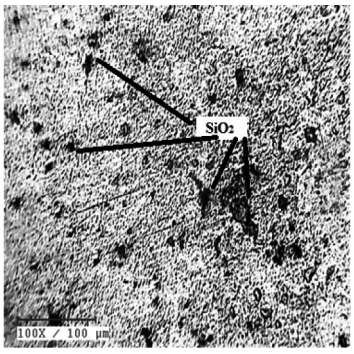

Fig. 2 Microstructure of AMC
2. ábra AMC mikroszerkezete

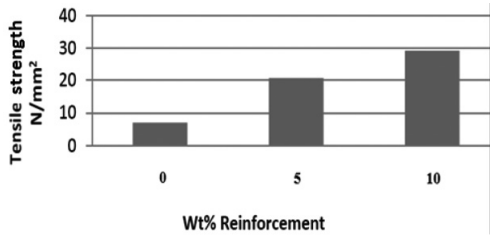

Fig. 3 Tensile strength vs wt % of SiO_2
3. ábra Húzószilárdság SiO_2 tartalom függvényében

As a result of this effect on hardness, it was determined that the value of hardness is better with increased traction. It is also noted that the maximum hardness is attained at Al with 10 wt% SiO_2. The hardness cost of pure Al turned into 26 BHN, which became elevated to 30 BHN with the addition of five wt.% SiO_2 within the Al matrix and 33 BHN for 10 wt.% SiO_2.Improvement of hardness value is achieved for 5 wt% SiO_2 is 15% and similarly, for 10 wt%, SiO_2 is 26%. Increase of the hardness value shows that the addition of silica particles increased to 10%, the hardness increased. This is because the harder SiO_2 particles replace some of the soft Aluminum. However, when the addition of reinforcement increased beyond 10 wt%, the hardness decreased. This is because more silica particle presents in the Al matrix then the bonding becomes poor. Hence beyond the addition of 10 wt% SiO_2 into Al matrix lead to low hardness. *Fig. 4* demonstrates the hardness estimations of the ALMMC. Uniform distribution of SiO_2 into Aluminum matrix would increase hardness and also ductile Aluminum would become a little bit brittle.

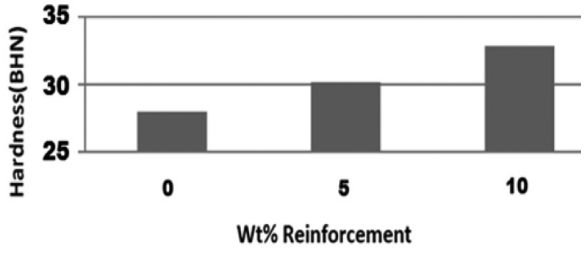

Fig. 4 Hardness vs wt % of SiO_2
4. ábra Keménység SiO_2 tartalom függvényében

The results confirms that 5 wt.% $SiO_2$with aluminium composites gives the yield strength of 22 N/mm^2 which is 100% higher than yield strength of pure aluminium (11 N/mm^2). Similarly, for 10 wt.% SiO_2, the yield strength is 28 N/mm^2, which gives an improvement of 154% compared to unreinforced Al. *Fig. 5* shows the yield strength of the metal matrix composites. The uniform dissemination of SiO_2 in the aluminum lattice essentially improved the yield quality. *Fig. 6* shows that at 5% by mass of SiO_2, a decrease of 5%, 5% by SiO_2 and 3.7% at 10% by mass of SiO_2 is observed, while at 5% by mass of SiO_2 and 10% by mass, a decrease in SiO_2 is achieved using unreinforced Aluminum reaches 80%. Because of warm confound, the Al grid enters the stress state, and SiO_2 particles enter the compression state. Since SiO_2 has low elasticity and a high decrease in compressive quality is accomplished. It was noted that the newly created unaltered aluminum was strengthened by 10 wt. % SiO_2 has high resistance. Since it is very durable, conventional machining may not be suitable for machining operations. Therefore, the experiments were carried out in wire-cut EDM (EDM DK7740), which is shown in *Fig. 7*. Specifications of WEDM machine are given in *Table 2*. Molybdenum wire (DK7740) is used as the electrode wire in the EDM for wire cutting. To ensure a smooth movement of the wire feed, digital circuits controlled by an inverter are used. This molybdenum wire can be used for quite a long time with high accuracy and can reduce wire breakage. The width of the molybdenum wire used in this machining was 0.18 mm. EDM molybdenum cutting machines are mainly used in electrical products, automotive components, military industry, etc. Water is utilized to control resistivity and other electrical properties. Due to the high-temperature discharge, the dielectric cleaning fluid removes the surface that melts and the particles that are cut [13].The research sequence was carried out on WEDM machine [14]. The selected criteria for the preparation of productivity were MRR and it can very well be represented (equation 1) as the ratio of the difference in weight during handling to the time and thickness of the composite [15]. Readings were recorded using the extended scale.

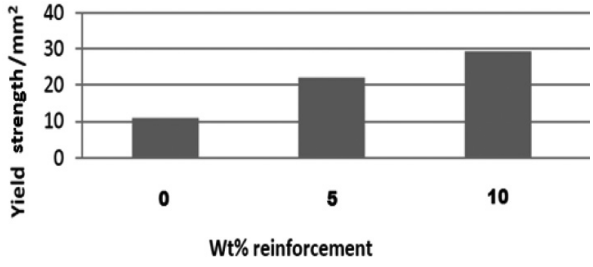

Fig. 5 Yield strength vs wt % of SiO_2
5. ábra Hajlítószilárdság SiO_2 tartalom függvényében

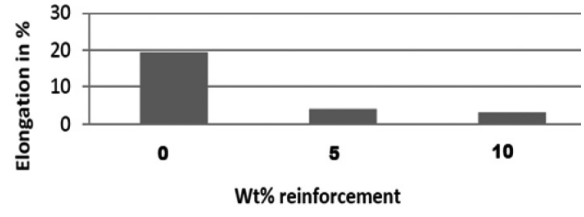

Fig. 6 Elongation vs wt % of SiO_2
6. ábra Megnyúlás SiO_2 tartalom függvényében

Fig. 7 Wire cut EDM machine
7. ábra Huzalos szikraforgácsoló gép

S.No	Item	Unit	DK7740
1	Travel of X/Y	mm	400 x 500
2	Table Size	mm	500 x 785
4	Maximum load of table	kg	500
5	Dimension (LxWxH)	mm	1700 x 1350 x 1700
6	Weight of machine	kg	2000
7	Best Finish	Ra≤μm	≤ 1.5

Table 2 Specifications of WEDM
2. táblázat WEDM eljárás műszaki adatai

$$MRR = (W_{ij}-W_{fj}) / (\rho_{composite} * t) \quad (1)$$

where W_{ij}&W_{fj} are the weights, t is the machining time.

To plan the experiments, Taguchi L9 orthogonal matrices were used. The Taguchi strategy is a procedure of value improvement, and this technique is utilized to lessen contrasts in item configuration and to improve quality. This strategy is known for its quality optimization [16]. Based on the trial configuration, tests were led, and the size of the chose piece was 10 mm. The test ought to be completed by changing the procedure parameters, which regularly influences the preparing procedure to get the required quality characteristics [17]. In this investigation, the Taguchi strategy is utilized to create orthogonal array (OA) for a sum of 3 parameters, namely pulse-on time,pulse-off time and current as shown in *Table 3*. The investigation expects to get a higher pace of material evacuation.In the present work, Analysis of Variance (ANOVA) was performed for a combined response variable using Minitab-19, statistical software and significant parameters responsible for the maximum MRR were listed in *Table 4*. It was found that the current has a significant effect (60.1%) on the MRR, followed by the pulse-off time (13%) and the pulse-on time (12%). The response data of the factor are presented in graphical form in *Fig. 8*. The best possible processing parameters are A1, B1 and C3. *Table 5* and *6* shows the reaction and ANOVA results respectively. By establishing the identified optimal values of the control parameters as input parameters (A1, B1 and C3), a control experiment is carried out using the same experimental setup and is repeated twice [18,19]. The values of the qualitative characteristics obtained during the verification experiments have an MRR of 16.1. The results of the validation tests are appeared in *Table 7*.

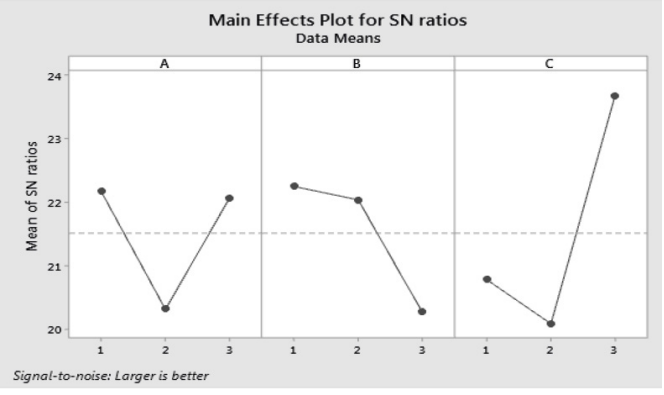

Fig. 8 Main effects plots for S/N ratios
8. ábra S/N arányok főbb hatásai

Parameters	Level-1	Level-2	Level-3
Pulse on time (μs)	6	7	8
Pulse off time (μs)	5	6	7
Current (A)	1	2	3

Table 3 Process parameters and their levels
3. táblázat Az eljárás paraméterei különböző szinteken

	Pulse on Time (μs)	Pulse off Time (μs)	Current (A)	MRR
1	6	5	1	13.9
2	6	6	2	9.99
3	6	7	3	15.2
4	7	5	2	10.2
5	7	6	3	15.3
6	7	7	1	7.13
7	8	5	3	15.3
8	8	6	1	13.2
9	8	7	2	10.1

Table 4 Experimental layout using L9 OA and performance result
4. táblázat Kísérleti elrendezések L9 OA felhasználása esetén és eredményeik

Level	A	B	C
1	22.16	22.24	20.78
2	20.31	22.03	20.08
3	22.06	20.26	23.67
Delta	1.85	1.98	3.59
Rank	3	2	1

Table 5 Response table for signal to noise ratios
5. táblázat Jel-zaj arányok válaszreakciós táblázata

Source	DF	Adj SS	Adj MS	F-Value	P-Value	%contribution
Pulse on time (μs)	2	8.624	4.312	0.90	0.526	12
Pulse off time (μs)	2	9.570	4.785	1.00	0.500	13
Current (A)	2	43.328	21.664	4.53	0.181	60.1
Error	2	9.557	4.779			
Total	8	71.079				

Table 6 Analysis of variance (ANOVA)
6. táblázat Varianciaanalízis (ANOVA)

S.No	Items	Initial cutting parameters	Optimal machining parameters	
			Prediction	Experiment
1	Level	A1B1C1	A1B1C3	A2B2C1
2	MRR	13.9	16.9	16.1
3	S/N ratio	22.8603	25.0557	24.1365

Table 7 Results of the confirmation test
7. táblázat Teszteredmények

4. Conclusion

Quartz sand waste discharged into the open area was collected and successfully used as reinforcement in a pure Aluminum matrix. In this study, a stir casting method was chosen for the manufacture of MMCs, as this is the cheapest manufacturing method used to make complex moulds. The mechanical properties of the newly manufactured Al / SiO_2 compounds improved significantly until the reinforcement level reached Al + 10% SiO_2. The hardness of pure Al was 26 BHN, increased to 30 BHN with the addition of 5% by weight of SiO_2 to the Al matrix and 33 BHN for 10% by weight of SiO_2. A rise in the hardness of 5 wt. % SiO_2 is 15%, and similarly for 10 wt. % SiO_2 is 26%. It was shown that the elastic limit of 5% by weight of SiO_2 showed an elastic limit of 100% higher. Similarly, for 10 wt. % SiO_2, the elastic limit is 28 N/mm^2, which provides an improvement of 154% compared with unreinforced Aluminum.The range of recovery results showed that a decrease of 4% for 5% by weight of SiO_2 and by 3.7% for 10% by weight of SiO_2.79% for a decrease of 5% by weight of SiO_2 and 80% reduction for 10% mass of SiO_2 with unreinforced Al.An optical microscope image shows that SiO_2 particles are well distributed in the Al matrix. It was concluded that Al with 10 wt. % SiO_2 can be considered as a suitable material in sectors where lightweight with improved mechanical properties is required. Therefore, Al + 10% by weight of SiO_2 obtained by casting with stirring are taken for Wire EDM cutting experiments.The current, which is the most significant parameter of 60.1%, gives a vital effect with a subsequent pulse-off time of 13% and the inclusion of a pulse on time of 12%. The percentage of errors (4.94) is in the acceptable range, which is less than 5%.

References

[1] Parswajinan, C. – Vijaya Ramnath, B. – Abishek, S. – Niharishsagar, B. – Sridhar, G. (2018): Hardness and impact behaviour of aluminium metal matrix composite. IOP Conference Series: *Materials Science and Engineering*, 390, 012075. doi:10.1088/1757-899x/390/1/012075.

[2] Saravanan, V. – Thyla, P. R. – Balakrishnan, S. R.: A Low Cost, Light Weight Cenosphere-Aluminum Composite for Brake Disc Application. *Bulletin of Materials Science 2016*, 39 (1), 299–305. https://doi.org/10.1007/s12034-015-1134-2.

[3] Vozniakovskii, A. – Kidalov, S. – Kol'tsova, T. (2019): Development of composite material aluminum-carbon nanotubes with high hardness and controlled thermal conductivity. *Journal of Composite Materials*, 53(21), 2959–2965. doi:10.1177/0021998319829894.

[4] Monich, P. R. – Romero, A. R. – Höllen, D. – Bernardo, E. (2018): Porous glass-ceramics from alkali activation and sinter-crystallization of mixtures of waste glass and residues from plasma processing of municipal solid waste. *Journal of Cleaner Production*, 188, 871–878. doi:10.1016/j.jclepro.2018.03.167

[5] Ihom, P. A. – Anbua, O. O. – Ogbodo, E. E.: Solid Waste Management : The Use of Broken Waste Bottles as Reinforcement Agent for Aluminum Matrix Composite. *International Journal of Science and Technology* 2012, 1 (10), 546–551.

[6] Sahu, M. K. – Sahu, R. K. (2018): Fabrication of Aluminum Matrix Composites by Stir Casting Technique and Stirring Process Parameters Optimization. *Advanced Casting Technologies*. doi:10.5772/intechopen.73485.

[7] Subrahmanyam, M. – Nancharaiah, T. (2019): Optimization of process parameters in wire-cut EDM of Inconel 625 using Taguchi's approach. *Materials Today: Proceedings*. doi:10.1016/j.matpr.2019.05.449

[8] Saravana Kumar, M. – Begum, S. R. – Vasumathi, M. (2019): Influence of stir casting parameters on particle distribution in metal matrix composites using stir casting process. *Materials Research Express*, 6(10), 1065d4. doi:10.1088/2053-1591/ab4045.

[9] Jana, S. – Mishra, R. S. – Grant, G. J. (2016): Friction Stir Processing. Friction Stir Casting Modification for Enhanced Structural Efficiency, 5–27. doi:10.1016/b978-0-12-803359-3.00002-9..

[10] MallikarjunaDuraipandian, M – Muthukannan, R. (2019): Determination of Mechanical Properties and Microstructure of the Aluminium/Fe2O3/B4C Composite Using Stir Casting Route. doi:10.7546/crabs.2019.04.12

[11] Chatterjee, S. – Mallick, A. B. (2012): Challenges in Manufacturing Aluminium Based Metal Matrix Nanocomposites via Stir Casting Route. *Materials Science Forum*, 736, 72–80. doi:10.4028/www.scientific.net/msf.736.72

[12] Jacob, S. S. G.: Thermal Analysis on Al7075/Al2O3 Metal Matrix Composites Fabricated by Stir Casting. IOP Conference Series: *Materials Science and Engineering* 2017, 183 (1), 1–8. https://doi.org/10.1088/1742-6596/755/1/011001

[13] Gopalakannan, S. – Senthilvelan, T.: Optimization of Machining Parameters for EDM Operations Based on Central Composite Design and Desirability Approach. *Journal of Mechanical Science and Technology* 2014, 28 (3), 1045–1053. https://doi.org/10.1007/s12206-013-1180-x

[14] Selvarajan, L. – Narayanan, C. S. – Jeyapaul, R.: Optimization of EDM Hole Drilling Parameters in Machining of MoSi 2 -SiC Intermetallic / Composites For. *Journal of Advanced Manufacturing Systems* 2015, 14 (4), 259–272. https://doi.org/10.1142/S0219686715500171

[15] Satishkumar, D. – Kanthababu, M. – Saravanan, R. – Moorthy, T. – Saravanan, P.: Optimization of Wire EDM Parameters on Machining of Al7075 Based Hybrid MMCs. *Advanced Composite Letters* 2012, 21 (4), 100–106. https://doi.org/10.1177/096369351202100403

[16] Phate, M. R. – Toney, S. B. – Phate, V. R.: Analysis of Machining Parameters in WEDM of Al/SiCp20 MMC Using Taguchi-Based Grey-Fuzzy Approach. *Modelling and Simulation in Engineering* 2019, 2019, 13. https://doi.org/10.1155/2019/1483169

[17] Durairaj, M. – Sudharsun, D. – Swamynathan, N.: Analysis of Process Parameters in Wire EDM with Stainless Steel Using Single Objective Taguchi Method and Multi-Objective Grey Relational Grade. *Procedia Engineering* 2013, 64, 868–877. https://doi.org/10.1016/j.proeng.2013.09.163

[18] Aherwar, A. – Singh, A. – Patnaik, A.: Mechanical and Wear Performance Evaluation of Tungsten Added Co-30Cr-4Mo-1Ni Biomedical Alloy with Taguchi Optimization. *Materialwissenschaft und Werkstofftechnik* 2018, 49 (7), 912–927. https://doi.org/10.1002/mawe.201700063

[19] Kasdekar, D. K. (2015): MADM Approach for Optimization of Multiple Responses in EDM of En-353 Steel. *International Journal of Advanced Science and Technology*, 83, 59–70. doi:10.14257/ijast.2015.83.06.

Ref.:
Kumaravel, Subramaniam – **Alagumurthi**, Natarajan: *Material removal characteristics of Al-SiO_2 composite in WEDM*
Építőanyag – Journal of Silicate Based and Composite Materials, Vol. 72, No. 1 (2020), 20–24. p.
https://doi.org/10.14382/epitoanyag-jsbcm.2020.4

Superficial hardening improvement of nano and micro composite Al TiC

Abderraouf GHERISSI ▪ Department of Mechanical Engineering, Faculty of Engineering, University of Tabuk, KSA - Saudi Arabia ▪ gherissi.abderraouf@gmail.com

Malik ALI ▪ Department of Mechanical Engineering, Faculty of Engineering, University of Tabuk, KSA - Saudi Arabia ▪ malikali77@yahoo.com

Érkezett: 2019. 11. 13. ▪ Received: 13. 11. 2019. ▪ https://doi.org/10.14382/epitoanyag-jsbcm.2020.5

Abstract

The present investigation aims to study the improvement of the composite surface hardness by air abrasive jet polishing (AJP) of SiO_2 particles. The experiments were conducted by synthesizing Al-TiC composites through melting the aluminum at 850°C and added TiC gradually for 10 minutes to the liquefied aluminum with different sizes and ratios (300-500 nm and 100-200 μm) and (5, 10, 15, 20 and 25 wt.%) respectively of TiC. The molten Al-TiC was poured to a previously prepared sand mould. The hardness improvement for pure Aluminum, Al- micro-TiC and Al- nano-TiC composites were 7%, 11%, and 15% respectively. The obtained results demonstrate the importance of superficial hardening of composites Al-TiC by impact of the SiO_2 air jet and show that the surface hardness improvement is greatest for the nanocomposites compared with micro-composite and pure matrix material.

Keywords: abrasive jet polishing, nano and micro composites Al-TiC, hardness improvement, SiO_2
Kulcsszavak: csiszolófúvós polírozás, Al-TiC nano és mikro kompozitok, keménység növel, SiO_2

Abderraouf GHERISSI
Assistant Professor of Mechanical Engineering at the Mechanical Engineering Department, College of Engineering, University of Tabuk in Saudi Arabia. Actually involved in several research projects in the field of Composite materials, advanced production process and clean energy.

Malek ALI
Associate Professor, Department of Mechanical Engineering, University of Tabuk, Tabuk, Saudi Arabia. Research experience in the following areas: Synthesis Advanced Nanomaterials, Metallurgy, Nano. Composites (Polymer, Ceramics, Metals), Corrosion and Energy Manufacturing/Fabrication of Metallic.

1. Introduction

The surface finish of Al-TiC components plays an important role in the mechanical response and wear resistance. Therefore, the surface treatment is a primordial process to achieve certain qualities that are not available from the primary manufacturing processes. One of the effective surface treatment processes is the polishing process using abrasive jet of particles. The effect of polishing techniques and penning on surface roughness and hardness are widely studies on composites [1]. Abrasive jet machining (AJM) is a process that does not include a physical contact between the tool and work piece so there are no thermal stresses and shocks developed. AJM can be used for many processes such as cutting, cleaning, polishing, etching, drilling and finishing operations. The effects of polishing techniques on surface roughness and micro hardness of resin composites are desirable in order to reduce the number of clinic sessions and bringing more comfort and satisfaction to the patient in dental application [2-4]. In addition, the air abrasion is commonly used on surface treatment for porcelain veneers [5]. The effect of different air-abrasion particles on metal-ceramic bond strength is widely analyzed in the work of Tolga Kulunk et al. [6]. Other studies using abrasive water jet polishing were conducted to improve the fatigue strength of metals [7, 8]. F. Boud et al. [9] studied the impact of plain water jet machining on the surface integrity of aluminum 7475. Others focused on penning treatment such as Kyun-Taek Cho et al. [10] who worked on surface hardening of aluminum alloy by soft-shot polishing treatment with Zn based ball. In this work, a nano and micro composites of Al-TiC are chosen as testing materials. Several previous works have been done in the synthesis of Al-TiC composites [11, 12]. In an attempt to improve the Al-TiC composites surfaces hardness with different TiC sizes and ratios a high efficient and low-cost AJP machine is designed to conduct the proposed testing.

2. Experimental procedures

Aluminum (Al) was used as matrix material whereas TiC particles with different sizes and ratios (300-500 nm and 100-200 μm), (5, 10, 15, 20 and 25wt. %) were used as reinforcement in the Al-TiC composites. Melting of Al was carried out using a resistance furnace operating at 850°C. The reinforcements were then added gradually for 10 minutes to the molten aluminum with different weight ratios (5, 10, 15, 20 and 25) wt.% of TiC. Mixtures were stirred for 10 minutes after the additions of TiC. The stirrer rod was operated at 450 rpm to ensure a good distribution and homogeneity of the nano and micro TiC powder in the molten Al matrix. With 10 °C/min heating rate the furnace, the temperature was held at 850°C to ensure high fluidity of Al. After the Al-TiC became homogenous, the liquefied Al-TiC was poured in to previously prepared sand mould. However, at a temperature of 700°C the molten became in a semi-solid state, where the slurry cannot be poured into the mold because at this stage, its viscosity is high and the fluidity is greatly low. Therefore, before pouring the slurry into the mold, it was necessary to re-melt it to a molten condition, and re-stir before pouring [13]. The abrasive jet machine (AJM) is utilized in the unconventional machining process of material removal from a work piece by the application of a high speed stream of abrasive particles carried in the air medium from a nozzle as shown in *Fig. 1*.

The AJM is used to cut hard and brittle materials where a three-axis CNC machine is utilized for material removal process. The machines are designed and selected through appropriately to o the tasks. To design and construct the AJM components several factors have to be considered: compressible flow law, carrier gas, flow rate, vibration level, nozzle size, stand-off effects, material removable rate estimation, etc. The

selection of parts, the assembly process, the fabrication and the test of the machine performance were carried out. The AJM was designed and constructed to perform a CNC engraving, cutting and drilling as shown in *Fig. 2*.

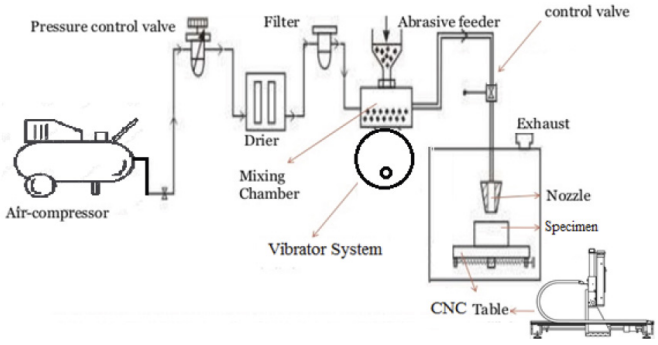

Fig. 1 Schematic representation of the AJM
1. ábra AJM sematikus ábrázolása

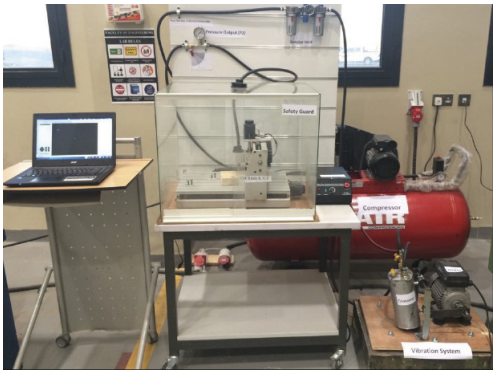

(a)

(b)

Fig. 2 The abrasive jet machine (AJM) (a), the nozzle (b)
2. ábra AJM (a), fúvóka (b)

The AJP was designed with abrasive Silica sand (SiO_2) and used with a 90° impact angle and average gas pressure of around 5 bar with 2 mm nozzle diameter and a standoff height of 10 mm. The mass flow rate of SiO_2 was set to 1.2 gram/s. Total polishing time was 10 seconds. Control of the nozzle position and the blasting time on the top surface were controlled by a CNC table. Hardness test evaluation was carried out through the Brinell test machine WP 300 from GANT Company. Brinell hardness test carried out at 9.8 KN for 30 seconds. The test was used to investigate the influence of sizes and weight fraction of TiC on the matrix hardness. A total of five samples were taken for each ratio of the Al-TiC to obtain the average hardness value for an accurate result. The concept of hardness improvement by abrasive jet polishing of SiO_2 particles is represented in *Fig. 3*. The Silica sand SiO_2 particles are characterized by a large number of irregular angular surface features and have a relatively high hardness (Mohs Hardness 6-7).

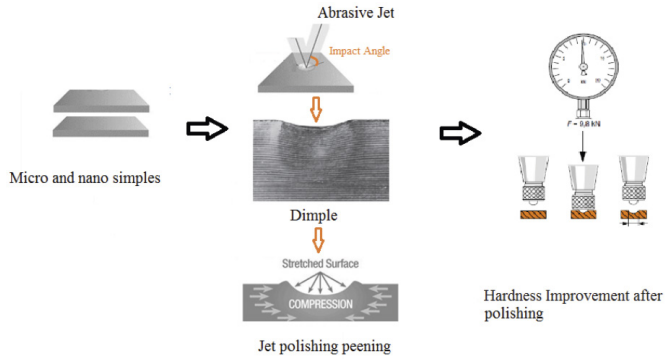

Fig. 3 The concept of hardness improvement by abrasive jet polishing of SiO_2
3. ábra A keménység növelésének koncepciója SiO_2 csiszolófúvós polírozásával

In order to evaluate the efficiency of the abrasive polishing machine, a primary experiment was carried out on four known specimens delivered from GANT Company under standard references as shown in *Table 1*. The polishing test was performed using aluminum alloy EN AW-6082 (called in ISO: Al Si1MgMn), copper CW004A (designation for the 99.9% pure copper), Brass CW614N with 37-45% Zinc, steel alloy S235 – IAC-C with maxi C% of 0.22 and Mn % of 1.6.

Based to the experimental results grouped in *Table 1*, it is observed that the increasing of the hardness of the aluminum alloy is about 51%, for the copper alloy is 73%, for brass is 53% and for steel is 29%. The improvement of surface hardness was significant, which confirm the effectiveness of the present jet polishing process on the material surface finishing.

Material	Brinell Hardness before polishing	Brinell Hardness after polishing t*=10s d*= 10 mm Polishing at MP=1.2 gram/s	Percentage of hardness improvement MP*=1.2 gram/s
Aluminum Alloy EN AW-6082	67 HB	101 HB	51%
Copper Alloy CW004A	55 HB	95 HB	73%
Brass CW614N	90 HB	138 HB	53%
Steel S235-IAC-C	130 HB	168 HB	29%

**t(s): Time of polishing.*
**d (mm): Standoff distance between nozzle and top surface of the workpiece.*
**MP (gram/s): Mass flow rate of abrasive particle of SiO_2*

Table 1 Hardness improvement of standard specimens by polishing test
1. táblázat A minták keménységének növekedése polírozási teszt alapján

3. Results and discussion

3.1 Hardness results before polishing

In this part, hardness test was conducted to investigate the influence of sizes and weight fraction of TiC on the matrix

hardness. A total of five samples were taken for each ratio of Al-TiC to obtain the average hardness value for an accurate result. The hardness values of the micro and nano composites depend on the amount of particles, sizes, and uniformity distribution of TiC particles in the Al matrix as shown in *Fig. 4*.

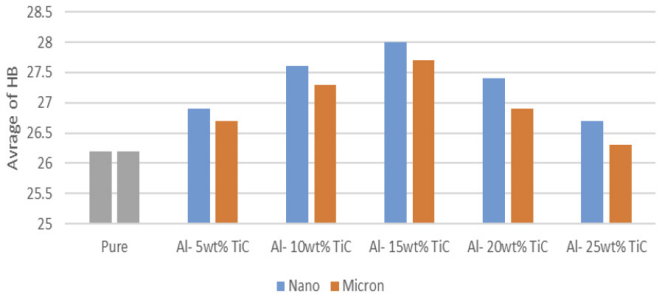

Fig. 4 Comparison between average HB for nano and micro
4. ábra Átlagos Brinell-keménység összehasonlítása nano- és mikro kompozitokon

It is observed from the results of hardness in *Fig. 4* that all reinforced specimens have a higher hardness than that of the matrix material. In general, the hardness increases with increasing the hard particles (TiC). The hardness for specimens with 20 wt% and 25 wt% TiC decreases due to the agglomeration of TiC particles. For these samples, the highest hardness measured is at 15 wt% Nano TiC at 28 HB while the minimum hardness is at 0 wt%, and that proves that the aluminum reinforced with TiC improves the hardness. Moreover, it was observed based on *Fig. 4* that the nano-particles of TiC gives a little higher hardness for the composite Al-TiC compared with micro particles. The decrease of hardness at 20 wt% and 25 wt% of TiC is due to the effects of grain boundary.

The presented results had been observed in several investigations, which indicated the decrease of hardness below a critical grain size [17], [18] and [19]. Both experiments and simulations in [20], [21] and [22] have also shown that the strength/hardness decreases with further grain refinement below the critical value. This indicates the occurrence of a shift in the dominated deformation mechanisms from dislocation-mediated plasticity to grain-boundary-associated plasticity such as grain-boundary sliding, grain-boundary diffusion and grain rotation. Due to the small size of powder (especially in nano powder) a change is evident in hardness value for each specimen. If a particle is dispersed in the composite, a better value for hardness would be obtained. The agglomeration that occurs affects the mechanical behavior of the specimen. This is due to the powder collected at one portion of the specimen that causes a soft and porous surface.

3.2 Hardness improvement after polishing of the composite Al-TiC

All specimens were tested for Brinell hardness before the polishing. The outer surfaces of the workpieces were machined using an abrasive jet at a standoff of 10 mm and mass flow rate of abrasive particles of 1.2 gram/s. Then, the Brinell hardness test was repeated again on the same specimens. The degree of surface roughness was changed and the hardness as well. The amelioration of the hardness of the nano and micro composite Al-TiC simples at different ratios of TiC are regrouped in *Table 2*.

The percentage rates of hardness improvement in specimens were calculated through five experimental tests on each specimen. The average is presented in *Table 2* for micro-composite and nano-composite with different ratios of TiC. By comparing the hardness before and after polishing it is clearly noticed that the increasing of hardness is about 7% to 15% for nanocomposites and about 6% to 11% for micro-composites due to the impact

of SiO_2 particles by abrasive jet polishing. This process produces tensile stresses in the surface because the surface is trying to become plastically larger.

As a reaction to the polishing or peening treatment a compressive unused stress is formed in the surface layer. These compressive unused stresses have to be balanced by unused tensile stresses in the entirely elastically deformed component interior.

Material specimen micro composites	Before polishing (HB)	After polishing (HB)	Percentage of hardness improvement
Pure Al	26.2	28	7%
Al- 5wt% TiC	26.7	28.7	7%
Al- 10wt% TiC	27.3	29	6%
Al- 15wt% TiC	27.7	30.7	11%
Al-20wt% TiC	26.9	29	8%
Al- 25wt% TiC	26.3	28.5	8%
Material specimen nano composites	**Before polishing (HB)**	**After polishing (HB)**	**Percentage of hardness improvement**
Pure Al	26.2	28.4	8%
Al- 5wt% TiC	26.9	28.8	7%
Al- 10wt% TiC	27.6	30.5	11%
Al- 15wt% TiC	28	32.3	15%
Al-20wt% TiC	27.4	31	13%
Al- 25wt% TiC	26.7	29	9%

Table 2 Hardness improvement for micro, and nano polishing Al- TiC composites
2. táblázat Az nano- és mikro polírozott Al-TiC kompozitok keménységének növekedése

The position of the maximum of compressive residual stresses depends on several parameters such as: the compressible flow law, carrier gas, flow rate, vibration level, nozzle size, stand-off effects, material removable rate estimation, etc. With increasing the shot peening time, deeper surface layers are plastically deformed, until a saturation is reached, which depends on the energy of the impact shot. The surface shows an increased dislocation density and roughness after shot polishing as in *Figs. 5(b)* and *6(b)*. This increase in the dislocation density leads to an increase in the material strength of the surface. This hardening of the polishing Al-TiC composite surfaces have been easily proven by Brinell hardness as shown in *Table 2*. In addition, it is noticed that the hardness decreases after

reaching 15 wt% of TiC in the aluminum matrix due to the high content of TiC in the Al matrix, which is very sensitive to the agglomeration of TiC.

3.3. Microstructure Image Analyses

The micrographs shown in *Figs. 5(a)* and *6(a)* clearly display the distribution of the TiC particles (dark areas) in the Al matrix (bright areas). As shown in *Figs. 5(a)* and *6(a),* the small particles are distributed homogenously among the big particles (agglomeration of many small particles together). It should be noted that the particle sizes of the small particles are uniformly distributed. However, some pores can be observed. The formation of pores is mainly due to the non-uniformity of the initial TiC particles. Moreover, it is clear from *Figs. 5(a)* and *6(a)* that the reinforcement particles of the composites are embedded in the aluminum matrix. A small agglomeration of TiC particles in the aluminum matrix has been noticed, and this is mainly due to the non-homogeneity involved in the mixing process carried out before casting. The size of the TiC particles in the composites increases as the TiC content increases.

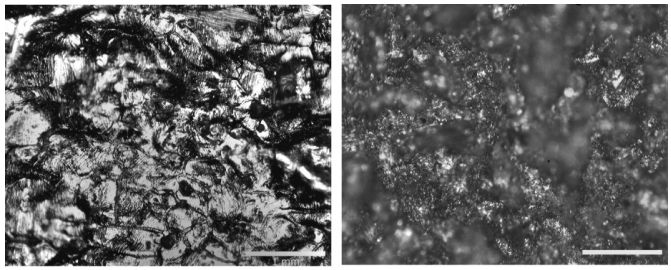

(a) (b)

Fig. 5 Microscopic observation of the nanocomposite Al TiC at Wt 10% (a) before polishing and (b) after polishing
5. ábra Al TiC nanokompozitok mikroszkópos vizsgálata (a) polirozás előtt és (b) polirozás után

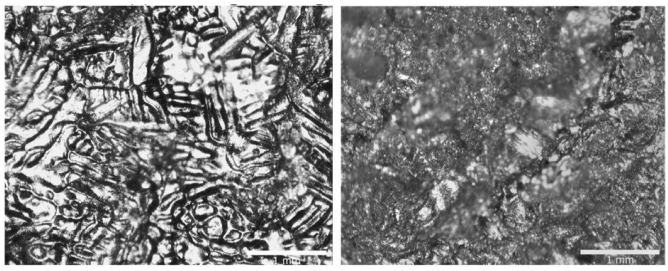

(a) (b)

Fig. 6 Microscopic observation of the microcomposite Al TiC at Wt 10% before polishing and (b) after polishing
6. ábra Al TiC mikrokompozitok mikroszkópos vizsgálata (a) polírozás előtt és (b) polírozás után

The surface shows an increased dislocation density and roughness after shot polishing as in *Figs. 5(b)* and *6(b)*. This increase in dislocation density leads to an increase in the porosity and material strength in the surface. The increase in roughness inherited during shot peening must always be considered as negative. At higher magnification overlaps, micro-cracks and areas with an obvious turbulent flow can be found. With the increase in peening time the surface roughness increases as well. A compressive residual stresses can be done to drastically reduce the faster crack propagation rate of the homogeneously deforming surface zone.

4. Conclusion

The presented study exposes the improvement of hardness for composites surfaces by Abrasive Jet Polishing (AJP). Composites of Al-TiC have been synthesized successfully by stir casting process with different sizes and ratios of TiC (300-500 nm, and 100-200 μm) and (5, 10, 15, 20 and 25 wt.%) respectively. An AJP by abrasive silica sand (SiO_2) was used to conduct the experiments. The increases in surface hardness for aluminum alloy, copper alloy, brass, steel were about 51%, 73%, 53%, and 29%, respectively. Hardness improvement for pure aluminum, Al-microTiC, Al-nanoTiC composites were 7%, 11%, and 15%, respectively. From the introduced results, improvements in polished surface workpiece are limited by the SiO_2 grain-impact phenomenon and the embedment of SiO_2 fragments in the workpiece surface. The surface shows an increased dislocation density and roughness after shot polishing. This increase in dislocation density leads to an increased porosity, material strength in the surface, and reduction the faster crack propagation rate of the homogeneously deforming surface zone. The obtained results on Al-TiC composite demonstrate the importance of superficial hardening of composites by impact of the SiO_2 air jet and show that the surface hardness improvement is greatest for the nanocomposites compared with micro-composite and pure matrix material.

References

[1] Chen, Fengjun – Miao, Xiangliang – Tang, Yu – Yin, Shaohui (2017): A review on recent advances in machining methods based on abrasive jet polishing (AJP), Int. J Adv Manuf Technol 2017,90:785–799. https://doi.org/10.1007/s00170-016-9405-7

[2] Venturini, D. – Cenci, M.S. – Demarco, F.F. – Camacho, G.B. – Powers, J.M. (2006): Effect of Polishing Techniques and Time on Surface Roughness, Hardness and Microleakage of Resin Composite Restorations, Operative Dentistry, 2006, 31-1, 11-17. https://doi.org/10.2341/04-155

[3] Kristine Guará Brusaca Almeida ScheibeI – Karoline Guará Brusaca AlmeidaI – Igor Studart Medeiros II – José Ferreira Costa III – Cláudia Maria Coêlho Alves (2009): Effect of different polishing systems on the surface roughness of microhybrid composites, J. Appl. Oral Sci. vol.17 no.1 Bauru Jan./Feb. 2009 http://dx.doi.org/10.1590/S1678-77572009000100005

[4] Michelle Alexandra Chinelatti – Daniela Thomazatti ChimelloI – Renata Pereira Ramos – Regina Guenka Palma-Dibb (2006): Evaluation of the surface hardness of composite resins before and after polishing at different times, J. Appl. Oral Sci. vol.14 no.3 Bauru 2006. doi - 10.1590/S1678-77572006000300008

[5] Aswal, G S – Nair, C K (2015): Effects of various parameters of alumina air abrasion on the mechanical properties of low- fusing feldspathic porcelain laminate material, SADJ 2015, Vol 70 no 4 p150 - p155

[6] Tolga Kulunk – Murat Kurt – C¸agrı Ural – S, afak Kulunk – Seniha Baba, (2011): Effect of different air-abrasion particles on metal-ceramic bond strength, Journal of Dental Sciences 2011 6, 140-1460. doi: 10.3109/00016357.2010.536907

[7] D. Arola – A. E. Alade – W. Weber,(2006): Improving Fatigue Strength of Metals Using Abrasive Waterjet Polishing, Machining Science and Technology, 10: 2006, 197–218. https://doi.org/10.1080/10910340600710105

[8] A. Azhari – S Sulaiman – A K Prasada Rao (2016): A review on the application of polishing processes for surface treatment, IOP Conf. Series: Materials Science and Engineering 114,2016 012002. https://doi.org/10.1088/1757-899X/114/1/012002

[9] F. Boud – L. F. Loo – P. K. Kinnell (2014): The Impact of Plain Waterjet Machining on the Surface Integrity of Aluminium 7475, Procedia CIRP 13, 2014 ,382 – 386. doi: 10.1016/j.procir.2014.04.065

[10] Kyun Taek Choa – Kyung Song – Sang Ho Oh – Young-Kook Lee – Kyoung Mook Lim – Won Beom Lee (2012): Surface hardening of aluminum alloy by shot polishing treatment with Zn based ball, Materials Science and Engineering A 543, 2012, 44–49. https://doi.org/10.1016/j.msea.2012.02.043

[11] Malek Ali – Ali Samer Muhsan – Projjal Basu – Faiz Ahmad1 (2013):Wear resistance of Al-12Si Alloys by Reinforcing TiC and TiN Particles. Journal of Engineering Mechanics (2013) 10.1061/(ASCE)EM.1943-7889.0000743. doi: 10.1061/(ASCE)EM.1943-7889.0000743

[12] Malek Ali – Samer Falih (2014): Synthesis and Characterization of Aluminum Composites Materials Reinforced with TiC Nano- Particles. Jordan Journal of Mechanical and Industrial Engineering, Volu. 8 No. 5, 2014, 244-250.

[13] Hashim, J. – Looney, L. – Hashmi, M. S. J. (1999): Metal matrix campsites: production by the stir casting method. Journal of Materials Processing Technology 1999, 92-93, 1-7.

[14] Chang, J. – Moon, I. – Choi, C.: Refinement of Cast Microstructure of Hypereutectic Al-Si Alloys Through the Addition of Rare Earth Metals, Journal of Materials Science (1998) 33: 5015. https://doi.org/10.1016/S0924-0136(99)00118-1

[15] Saeed Farahany – Hamidreza Ghandvar – Nur Azmah Nordin – Ali Ourdjini – Mohd Hasbullah Idris (2016): Effect of Primary and Eutectic Mg2Si Crystal Modifications on the Mechanical Properties and Sliding Wear Behaviour of an Al–20Mg2Si–2Cu–xBi Composite, Journal of Materials Science & Technology (2016), Pages 1083-1097. doi: 10.1016/j.jmst.2016.01.014

[16] M. Emamya – N. Nemati – A. Heidarzadeha (2010): The influence of Cu rich intermetallic phases on the microstructure, hardness and tensile properties of Al–15% Mg2Si composite, Materials Science and Engineering: A, Volume 527, Issue 12, 2010, Pages 2998-3004. https://doi.org/10.1016/j.msea.2010.01.063

[17] Yalçın, B. (2009): Effect of Porosity on the Mechanical Properties and WearPerformance of 2% Copper Reinforced Sintered Steel Used in Shock Absorber Piston Production,J. Mater. Sci. Technol.,2009 Vol.25 No.5.

[18] H. Conrad (2004): Grain-size dependence of the flow stress of Cu from millimeters to nanometers Metallurgical and Materials Transactions A, 35, 2004, pp. 2681–2695. https://doi.org/10.1007/s11661-004-0214-5

[19] C. Schuh – T. Nieh – T. Yamasaki (2002): Hall–Petch breakdown manifested in abrasive wear resistance of nanocrystalline nickel, Volume 46, Issue 10, 24 May 2002, Pages 735-740. https://doi.org/10.1016/S1359-6462(02)00062-3

[20] Hao Yin – Liu Pan – Qingping Sun (2017): Grain Size Effects on Wear Resistance of Nanocrystalline NiTi Shape Memory Alloy, 2017 Advances in Shape Memory Materials: In Commemoration of the Retirement of Professor Hisaaki Tobushi, vol - 73. doi: 10.1007/978-3-319-53306-3_16

[21] X. Li – Y. Wei – L. Lu – K. Lu – H. Gao (2010): Dislocation nucleation governed softening and maximum strength in nano-twinned metals Nature, 464,2010 , pp. 877–880. doi: 10.1038/nature08929.

[22] D. Wolf – V. Yamakov – S. Phillpot – A. Mukherjee – H. Gleiter (2005): Deformation of nanocrystalline materials by molecular-dynamics simulation: relationship to experiments? Acta Materialia, 53, 2005, pp. 1–40. https://doi.org/10.1016/j.actamat.2004.08.045

Ref.:
Gherissi, Abderraouf – **Ali**, Malik: *Superficial hardening improvement of nano and micro composite Al TiC*
Építőanyag – Journal of Silicate Based and Composite Materials, Vol. 72, No. 1 (2020), 25–29. p.
https://doi.org/10.14382/epitoanyag-jsbcm.2020.5

Creation of "necessary" mixtures of baking soda, hydrogen peroxide and warm water as a strategy for modernization bleaching cleaners of ceramic

Aleksandr L. URAKOV
is Professor, Leading Specialist in Udmurt Federal Research Center; Head of Department Pharmacology in Izhevsk State Medical Academy, author of 220 inventions. Honored inventor of the Russian Federation

Aleksandr URAKOV ▪ Udmurt Federal Research Center of the Ural branch of the Russian Academy of Sciences ▪ urakoval@live.ru

Érkezett: 2019. 10. 13. ▪ Received: 13. 10. 2019. ▪ https://doi.org/10.14382/epitoanyag-jsbcm.2020.6

Abstract

Hydrogen peroxide solutions have been used for more than 100 years as industrial bleach for various wood, paper, textile, leather products, as well as for hair whitening. Since the same time, hydrogen peroxide solutions and sodium bicarbonate solutions have been widely used in medicine as antiseptic and disinfectants to remove pus from purulent wounds. Less than this period, hydrogen peroxide solutions are successfully used for bleaching fish and various seafood. However, until the early 21st century, the combination of hydrogen peroxide with sodium bicarbonate was not used as a bleaching cleaner for surfaces contaminated with blood and/or pus stains. The use of hydrogen peroxide solution in combination with sodium bicarbonate as a universal bleaching and dissolving medical cleaner was first proposed in the last 20 years in Russia. It was during these years that a new group of drugs was discovered in pharmacology: drugs, bleaching and dissolving blood stains and a mass of thick pus. It is proved that the local application of various mixtures of baking soda, hydrogen peroxide and warm water provides a safe urgent dissolution and discoloration of the dense biological masses. It is established that purification, bleaching and removal of organic pollutants is achieved due to their hyperthermal softening, cavitation loosening, alkaline saponification and dissolution, as well as due to oxidative discoloration of pigments. It is proposed to use the created Arsenal of biomedical alkaline bleaching cleaners for the analysis and development of new effective and safe ceramic bleaches in everyday life.

Keywords: teeth, dentures, ceramic, hydrogen peroxide, sodium hydrogen carbonate, bleaching agent
Kulcsszavak: fogak, fogsorok, kerámia, hidrogén-peroxid, nátrium-hidrogén-karbonát, fehérítő

1. Introduction

One of the distinguishing features of high-quality ceramic tableware and many other ceramic, bioceramic, clay and metal products intended for storage, preparation and consumption of food products is the presence of enamel on their working surface. This enamel in its physical and chemical properties is very similar to the enamel that covers the working surfaces of mollusk shells, human and animal teeth. Such enamel is also covered of modern ceramic and/or metal-ceramic dentures and braces [1]. The common property of all these enamels is that they have a very high strength and a very smooth and slippery surface that does not even have a micropore. Therefore, the surface of these enamels has low adhesion to organic substances and microorganisms and is easily cleaned from dirt when washing [2]. In turn, the purity of the enamel surface affects the contamination of products and determines the aesthetic properties of the product [3].

In addition, the cleanliness of the working surfaces of the discussed products is the main task of sanitary and hygienic control of their quality. The fact is that the remains of food products, stuck to the surface of the enamel, can turn into a kind of fertile bed for the reproduction of microorganisms, of which some part can become a breeding ground for infectious diseases. Therefore, in practice, the contamination of surfaces is investigated not so much for the presence of food products on it, as for their contamination with microorganisms [4,5].

Therefore, it is no accident that wherever objects and products covered with enamel are used, hygienic means are constantly and repeatedly used to care for them, or rather-to clean the enamel surface from mechanical and microbiological contaminants. Therefore, at all times the production of ceramics and enamels has been inextricably linked with the production of disinfectants, detergents, bleaching and hygiene products [6].

In the second half of the 20th century, the world has increased interest in household ceramic products. In the late 20th century and early 21st century, the demand for ceramic and bioceramic medical products increased. Nowadays, the demand for ceramic products used in dentistry is especially great [7].

Due to the high demand for ceramic products, their quantity, range and quality has increased significantly. At the same time, the use of known detergents and devices (washcloths, sponges, wipes, mops, brushes, Soaps, shampoos, washing powders, washing machines, food processors, etc.), personal

hygiene products in the oral cavity (toothpastes, toothbrushes, toothpicks, elixirs, etc.) still does not allow you to quickly achieve whiteness and purity of the surfaces of enamels covering cookware, baths, sinks, ceramic tiles, as well as teeth and dental constructions [1,8]. Therefore, within a few days or weeks after the start of the use of ceramic products, their surface becomes dirty and remains dirty regardless of the quality of enamel and hygiene products. It impairs the appearance of household products (such as cups, dishes, pots, pans, knives), teeth, dentures, braces and causes bad breath in humans and animals [9]. All this encourages researchers to search for new more effective means of washing and whitening enamel covering ceramic products.

The analysis of known detergents and cleaning agents, devices and methods of their application was carried out. It is shown that most traditional technical solutions are based on the principle of mechanical cleaning of the enamel surface from food contamination [10]. However, the effectiveness and safety of known detergents and bleaching agents and methods of their application is still not completely satisfied with consumers. At the same time, progress in this direction has slowed. This is probably due to the fact that the potential of this principle is almost completely exhausted. That is why to optimize the search for new tools, it is proposed to pay attention to a different principle of washing and whitening enamels.

In particular, as a new principle of enamel cleaning, the principle of physical-chemical dissolution of adhesives is proposed, which bind together all the residues of organic substances into one dense biomass, visible to the eye and assessed as a stain of pollution. It is shown that this principle can be realized with the help of hydrogen peroxide solution, to which sodium bicarbonate and/or oxygen gas under excessive pressure are added in excess [11]. Such a solution provides urgent purification and bleaching of the enamel surface from biological pollutants due to alkaline saponification of protein and protein-lipid complexes, "explosive" loosening of biomass due to cold boiling caused by the release of gas (in particular, oxygen) inside this biomass, and oxidative destruction of light-absorbing double bonds in pigments [12-14]. In this case, such a cleaner is safe for the consumer, as it includes edible ingredients [15].

It is demonstrated that this principle is successfully implemented in medicine for urgent dissolution of thick purulent masses, sulfur plugs and dried blood [11]. For this purpose, special technologies for the local application of alkaline aqueous solutions of hydrogen peroxide heated to 37 – 42 °C, saturated with oxygen gas under increased pressure and sometimes supplemented with an insoluble material with frictional properties are proposed [16]. It is noted that these physical and chemical factors have long been considered very important in terms of physical and chemical sciences. However, further research into their use in the field of hygiene is needed in order to develop more effective and safe cleaning and bleaching agents suitable and safe for the treatment of ceramic products in the home.

At the same time, the influence of these and other physical and chemical factors on the removal of dirt from the surface of enamels of ceramic products is still insufficiently studied.

2. Materials and methods

Since 1999, the search for patents for inventions and scientific information on new means and methods of dissolution and removal of dense biological masses using physical and chemical factors of local interaction has been continuously conducted. The search strategy keywords were as follows: brushes, mops, brooms, washcloths, soaps, shampoos, laundry detergent, washing powder, bleach, cleaner, tooth cleaner, thick pus solvent, toothpaste, blood stain, pus, tattoo, plaque, tooth, denture, ceramic ware, textiles, ceramics, skin and bruise. Key words were limited to means and ways of using them for hygienic and aesthetic purposes.

The criteria for inclusion of a scientific source were limited to the availability of information about the invented drugs and/or methods of their application, which allow due to physical and chemical factors of local interaction to urgently dissolve, discolor and remove from the surface of the skin, textiles or enamel stains of dried or thick blood and / or pus. The criterion of exclusion from the article was the lack of information about the invented means and / or methods providing urgent dissolution, removal of blood stains and pus from the contaminated surface and its bleaching with a local single application. The risk of individual bias in judgments was reduced by relying on the essence of the invention as a generally accepted criterion of novelty. A total of 29750 sources of information were examined, of which only 25 inventions were evaluated for consideration.

3. Results and discussion

The results of the analysis of the available scientific and patent information have shown that today there is no known means and no ingredient included in the composition of known combined preparations, the use of which separately from each other would ensure the rapid dissolution and loosening of biological stains bonded by coagulated proteins of animal, vegetable or microbial origin [11]. At the same time, the combination of hydrogen peroxide solution with alkali represents a surprisingly very promising direction for the development of new detergents, cleaning and bleaching agents. It is shown that in the last 20 years a whole Arsenal of new medicines and technologies of personal hygiene was invented, which allow for 1-2 minutes to completely clean the surface, stained with blood and/or pus [12,18]. The new drugs are designed for urgent dissolution, loosening, removal and discoloration of thick biological masses such as thick pus, sulfur plug, lacrimal stone and dry blood crust [11]. Such means are intended mainly for the treatment of purulent diseases (such as peritonitis, pancreonecrosis, pleurisy, otitis), thrombosis of vascular catheters and veins, as well as for discoloration of the skin and nail plates in the area of bruises and hematomas. The analysis showed that these drugs are aqueous solutions, and their main ingredients are hydrogen peroxide and sodium bicarbonate in certain ratios and concentrations [16].

Today it is safe to say that the development of a new group of detergents and bleaching hygiene products began in Russia [11]. The first means were developed for dissolving and removing thick pus from purulent wounds. In particular, the

beginning of the patent for the first invention of this group of hygiene products begins officially with 29.12.2000. It was on this day that the patent application for the invention "Method of treatment of long-term non-healing wounds" (RU Patent 2187287) was registered. In this invention, for urgent cleansing of the wound from purulent necrotic masses, it was first proposed to irrigate the wound heated to 37 °C with a solution of 3% hydrogen peroxide, after which it was proposed to warm the wound surface to 42 °C. Then, in 2005, the invention "Method for treating pleural empyema cases" (RU Patent 2308894) was created. It was the second invention in which for urgent removal of pus from the pleural cavity it was recommended to introduce into the purulent mass a solution of an alkaline surfactant heated to 42 °C.

In 2006, patent applications were filed for inventions such as "Hyper-gassed and hyper-osmotic antiseptic mixture" (RU Patent 2331441) and "Method for peritoneal dialysis using gasified solution" (RU Patent 2336833). In these inventions as a solvent of thick pus, an aqueous solution of 2.7-3.3% hydrogen peroxide, 0.9-10.0% sodium chloride and gaseous carbon dioxide was proposed at an excess pressure of 0.2 ATM at +8 °C. The new drug had the ability to cold boil in the purulent mass, so it literally "blew up" a monolithic piece of thick pus.

In 2009 there was a publication about 3 inventions: "Softening agent for thick and viscous pus" (RU Patent 2360685), "Malchikov's method of removing bile calculus" (RU Patent 2367375) and "Methods of diagnostics and treatment of clotted hemothorax" by A. Y. Malchikov (RU Patent 2368333). They were proposed to dissolve thick pus, gallstones and blood clots with warm solutions of hydrogen peroxide and sodium bicarbonate.

These inventions created the basis for the modernization of developments in the future. And so it happened: in the following years, the first successes in the urgent washing of various surfaces from thick pus and blood stains due to physical and chemical dissolution and loosening of biological masses continued to improve. The list of new drugs has increased. Today we can assume that the results can be transferred to another field of activity. In particular, the experience of creating new cleaners for the field of medicine can be used to create new cleaners for enamel ceramic products used in the field of life. It is likely that the most useful may be the results achieved in our time in the development of a group of drugs, loosening blood crusts and dissolving and brightening blood stains.

The fact is that the most difficult to remove stains that occur on tooth enamel and ceramic dishes are formed due to coagulation, denaturation and/or drying of proteins and protein-lipid complexes [19]. Therefore, proteins play the role of a kind of biological glue that glues pigment particles into a conglomerate and firmly adheres it to the surface of the enamel. The sources of this natural "glue" are animal and vegetable products containing proteins and fats [4]. In addition to ready-made proteins, fats and oils, similar products of microbial processing of starch, sugar, fiber and other substances also participate in the bonding of organic substances [19]. The fact is that food is not sterile. Is not sterile and the surface of the enamel. Moreover, very often foods are pre-seeded with fungi (yeast) for culinary purposes.

It is also very important that the remains of food products after they are glued to the enamel always acquire a darker color, which rarely depends on the original color of the food. On the contrary, the transformation of color in an ordinary stain of enamel contamination is likely to be similar to the transformation of color in the mass of food eaten in the process of their movement in the gastrointestinal tract: the food eaten may consist of white products such as white bread, white starch, milk, cottage cheese and sugar, but the feces formed from them, normally acquire a dark brown color. In this regard, it is likely that the dark color of feces, plaque and stains on ceramic products (such as dishes) is determined by the microbiological process of processing food residues and the formation of conventional organic pigments.

It is no secret that the main pigment that stains feces and plaque in a dark brown color is the pigment stercobilin, which is formed as a result of enzymatic and microbial destruction of blood proteins and/or bile [17].

It is shown that the color of blood depends mainly on the color of red blood cells, the color of which, in turn, depends on the color of hemoglobin. It is believed that under the action of enzymes and microorganisms, hemoglobin is converted successively into verdoglobin, biliverdin, and then into bilirubin. Bile also contains the pigment bilirubin. Bilirubin is converted under the action of microorganisms first into urobilinogen, and then into stercobilin. Stercobilin is the pigment that gives "digested" foods a characteristic brown color [20].

It should be noted that people have long learned to remove from household items dark stains of animal and vegetable origin (they usually stain textiles, wool, paper, wood and leather). More than 100 years ago, wood ash and water passed through such ash were used for this purpose [21]. Today, specially designed washing powders and bleaching solutions are used for these purposes [22]. It was found that most of these solutions are aqueous solutions of hydrogen peroxide with special physical and chemical properties [23,24].

However, hydrogen peroxide has been used for more than 100 years for industrial washing and bleaching of various products of plant and animal origin, namely-wood, paper, textile, leather products [25]. At the same time, the safety of hydrogen peroxide for consumers of products bleached with this bleach was shown.

The experience of industrial application of hydrogen peroxide has shown that hydrogen peroxide is highly reactive, strong oxidizer and bleaching agent. It is shown that an increase in the concentration of hydrogen peroxide, an increase in the local temperature, an increase in the alkalinity of solutions above pH 7.0 and an increase in the duration of interaction enhances the bleaching effect of hydrogen peroxide. It was found that the bleaching effect of hydrogen peroxide increases the addition of compounds such as peroxosulfates, sodium peroxodisulfate, potassium peroxodisulfate, carbamine peroxide, ammonium peroxodisulfate, sodium carbonate, ammonia and silicate [23,24].

In addition, almost as many years hydrogen peroxide solutions are used for hair whitening.

In modern times, hydrogen peroxide is used to disinfect the water in which live fish swim [26], as well as to bleach seafood such as squid, octopus and cuttlefish [27]. It has been shown that fish remains safe for humans when ingested.

The fact that hydrogen peroxide is able to discolor various organic pigments, it became known to people also for a long time. In particular, in 1982, it was shown that the bleaching effect of hydrogen peroxide on hemoglobin is associated with hemolysis of erythrocytes and with the destruction of light-absorbing double bonds within colored pigments [28].

However, in the medical field, the first invention, which is a warm alkaline solution of hydrogen peroxide designed to discolor clothing stained with blood stains, was published in 2009. It was " a Method of rapid removal of blood stains from clothing" (RU Patent 2371532) [29].

Then in 2010, an article was published about a clinical case in which a urea gel containing 15% hydrogen peroxide minimized the discoloration and discomfort associated with ecchymosis [30]. It was shown that skin pigmentation in the area of ecchymosis was reduced due to the application of hydrated gel containing 5 to 20% hydrogen peroxide or urea peroxide to the skin during occlusion with an adhesive bandage.

In subsequent years, about 10 more drugs and methods were invented for urgent discoloration of the bloody bandage, skin and nail plate in the area of the wound, bruise and hematoma with solutions of 0.01-3% hydrogen peroxide and 1.7-10% sodium bicarbonate at a temperature of 37-42 °C [18]. Thus, during this period, the following inventions were developed: "Persons infrared differential express-diagnostics of bruising and injury of soft tissues" (RU Patent 2577510), "Bruise bleacher" (RU Patent 2539380), "Bleaching agent" (RU Patent 2589682), "Agent for intradermal bruise whitening" (RU Patent 2573382), "Method of skin discoloration in the area of bruising" (RU Patent 2582215), "Method for skin discoloration in bruising area" (RU Patent 2586278), "Method of removing paint from skin" (RU Patent 2600504), "Method for emergency bleaching and blood crust removal from skin in place of squeezed out acne" (RU Patent 2631593), "Means for intravital skin whitening near blue eyes" (RU Patent 2639485), "Method for whitening of bruise under eye" (RU Patent 2639283), "Bleaching opener of dried blood for wrapping bandages adhered to a wound" (RU Patent 2653465), "Decolorant of blood" (RU Patent 2647371), "Method for whitening of sore under nail" (RU Patent 2631592), "Method for blue nail treatment" (RU Patent 2641386) and "Method of emergency bleaching of the skin hematoma under the eye" (RU Patent 2679334).

The materials of these inventions prove that warm alkaline solutions of 0.1-3.0% hydrogen peroxide at pH 8.5 are unsurpassed leaders in bleaching fresh, dry and old blood.

Analysis of the composition of the invented bleach bruises and hematomas showed that the preparations of this new group of funds differ from all known detergents following properties [11]:

1. The main ingredients of bruise bleach are water, hydrogen peroxide and sodium bicarbonate.
2. Water, hydrogen peroxide and sodium bicarbonate are safe substances.
3. All bruise, hematoma and blood stain bleaches are alkaline oxidizers and have a pH of 8.5.
4. Bruising bleaches are applied locally at a temperature of 37-42 °C.
5. Water, hydrogen peroxide and sodium hydrocarbonate when absorption into the blood do not cause poisoning.

Independent studies show that solutions of hydrogen peroxide and sodium bicarbonate are fairly stable [31].

To date, it has been found that the mechanism of local action of alkaline bleaching oxidants is as follows:

- with local action, they have the ability of alkaline saponification of proteins and protein-lipid complexes,
- they have the ability to destroy biological masses from within due to the process of cold boiling
- they have the ability to destroy the light-absorbing double bonds inside the colored pigments.

It is known that hydrogen peroxide solutions as a bleaching drug are safe for people [32]. Therefore, a solution of 3% hydrogen peroxide is sold in pharmacies without a prescription as a local antiseptic, a solution of 5% hydrogen peroxide is used for hair whitening, a solution of 6.5% urea peroxide is used as an over-the-counter softener of earwax, and a solution of urea peroxide at a concentration of 5-20% is widely used in dentistry for teeth whitening [33,34]. In turn, sodium bicarbonate is an edible substance and is used in cooking under the name "baking soda".

It should be noted that following the discovery of thick pus solvents and bleach bruises and blood stains were invented tools that can completely remove plaque from the surface of the teeth and ceramic dental structures in a few tens of seconds after the start of local interaction. So, in 2017, a patent for the invention "Frictional toothpaste" (RU Patent 2626669) was issued. In this invention, for the urgent removal of dental plaque, a solution of 9.5-10% sodium bicarbonate and 0.5-1.5% hydrogen peroxide was first proposed, which in a ratio of 5/1 mass is poured into crystalline sodium bicarbonate at a temperature of +25 - +26 °C. As a result, a thick paste is formed, in which soft sodium bicarbonate crystals have abrasive, frictional, adhesive, erasing, absorption and adhesive activity against the rough and soft surface of the "tooth" dirt, but not against the smooth and hard surface of the tooth enamel and the smooth surface of the gum mucosa. On the other hand, the solution due to the dissolved part of sodium bicarbonate causes alkaline hydrolysis of proteins and saponification of fats, and due to hydrogen peroxide as a result of the catalase reaction releases oxygen gas, the bubbles of which cause the effect of cold boiling and destruction of biological masses.

Then in 2018, a patent was obtained for the first "Bleaching cleanser of dentures" (RU Patent 2659952). The invented bleaching agent is an aqueous solution of 3% hydrogen peroxide and 2-10 % sodium bicarbonate, which contains oxygen gas under an excess pressure of 0.2 ATM at +8 °C. Before use, this drug is heated to a temperature of 37-42 °C. It is shown that the developed drug in a few seconds after the beginning of local interaction with dirty teeth, dentures, ceramic utensils and surgical instruments completely and automatically

cleans, deodorizes and whitens their surface. Purification and bleaching is achieved by hyper temperature softening, alkaline saponification, cavitation loosening, dissolution and oxidative discoloration of various biological masses.

Thus, heated to 42 °C and saturated with oxygen gas under excessive pressure, aqueous solutions of 0.01-3% hydrogen peroxide and 1.7-10% sodium bicarbonate are automatically converted into strong detergents and bleaching agents. Such means are capable at single application within one minute automatically to clear enamel from a dental plaque, the rests of food, traces of pus, blood stains and from pollution by other biological products. At the same time, these bleaching agents remain safe. What's more, they are edible! (*Fig. 1*)

Fig. 1 Oxygen, used as a bleaching agent
1. ábra Oxigén, mint fehérítőszer

4. Conclusions

From the end of 2000 to the present time, more than 20 drugs and methods of their application in the medical field have been invented for emergency dissolution and discoloration of dense biological masses bonded by protein and protein-lipid complexes of blood and pus as a result of their coagulation and/or drying. Analysis of the composition of these preparations showed that all of them are aqueous solutions of 0.01-3% hydrogen peroxide and 1.7-10% sodium bicarbonate, heated to a temperature of 37-42 °C. It is shown, that the additional introduction of oxygen gas, carbon dioxide or other gases under excessive pressure, or insoluble sodium bicarbonate powder enhances and accelerates the washing and bleaching effect of these mixtures. It is established, that the mechanism of washing and bleaching action of such mixtures is that they have alkaline saponification of protein and protein-lipid complexes, the formation of gas bubbles at cold boiling and oxidative destruction of light-absorbing double bonds inside the colored pigments. It is proposed to use the experience of development and the existing Arsenal of new medical alkaline bleaching cleaners blood stains and pus for the analysis and development of new effective and safe bleaching cleaners ceramics in the home.

References

[1] Madfa, A. A. – Yue, X-G.: Dental prostheses mimic the natural enamel behavior under functional loading: A review article. Jpn Dent Sci Rev. 2016 Feb; 52(1): 2–13. https:// doi.org./10.1016/j.jdsr.2015.07.001.

[2] Dorthé E. – Zhang Y.: Load-bearing increase in alumina evoked by introduction of a functional glass gradient. Journal of the European Ceramic Society. 2012; 32 (6): 1213-1220. https://doi.org/10.1016/j.jeurceramsoc.2011.11.041.

[3] Fralick M. – Thomspson A. – Mourad O.: Lead toxicity from glazed ceramic cookware. CMAJ. 2016;188(17-18): E521–E524. https://doi.org/10.1503/cmaj.160182.

[4] Alum E.A. – Urom S.M. – Otu C. – Ben C. M. A.: Microbiological contamination of food: The mechanisms, impacts and prevention. International Journal of Scientific & Technology Research. 2016; 5 (03): 65-78. http://www.ijstr.org/final-print/mar2016/Microbiological-Contamination-Of-Food-The-Mechanisms-Impacts-And-Prevention.pdf. [Last accessed on 2019 Nov 19].

[5] Tamburini E. – Donegà V. – Gabriella M.M. – Pedrini P. – Monticelli C. – Balbo A.: Study on microbial deposition and contamination onto six surfaces commonly used in chemical and microbiological laboratories. Int J Environ Res Public Health. 2015; 12(7): 8295–8311. https://doi.org/10.3390/ijerph120708295.

[6] Barker J. – Naeeni M. – Bloomfield S.F.: The effects of cleaning and disinfection in reducing Salmonella contamination in a laboratory model kitchen. J. Appl. Microbiol. 2003; 95 (6): 1351-1360. https://www.ncbi.nlm.nih.gov/pubmed/14633010.

[7] Shenoy A. – Shenoy N.: Dental ceramics: An update. J Conserv Dent. 2010 Oct-Dec; 13(4): 195–203. https://doi.org/10.4103/0972-0707.73379.

[8] Tumwebaze I.K. – Hans-Joachim Mosler H-J.: Shared toilet users' collective cleaning and determinant factors in Kampala slums, Uganda. BMC Public Health. 2014; 14: 1260. https://doi.org/10.1186/1471-2458-14-1260.

[9] Aylıkcı B.U. – Çolak H. Halitosis: From diagnosis to management. J Nat Sci Biol Med. 2013; 4(1): 14–23. https://doi.org/10.4103/0976-9668.107255.

[10] Naseem, S. – Fatima S.H. – Ghazanfar H. – Haq S. – Khan N.A. – Mehmood M. – Ghazanfar A.: Oral hygiene practices and teeth cleaning techniques among medical students. Cureus. 2017; 9(7): e1487. 10.7759/cureus.1487.

[11] Urakov A. – Urakova N. – Reshetnikov A.: Oxygen alkaline dental's cleaners from tooth plaque, food debris, stains of blood and pus: A narrative review of the history of inventions. Journal of International Society of Preventive & Community Dentistry. 2019; 9 (5): 427-433. 10.4103/jispcd.JISPCD_296_19.

[12] Urakov A. – Urakova N. – Chernova L.: Possibility of dissolution and removal of thick pus due to the physical-chemical characteristics of the medicines. Journal of Materials Science and Engineering B. 2013;3(11):714 – 720. https://doi.org/10.17265/2161-6221/2013.11.005.

[13] Urakov A. L. – Urakova N. A. – Alies M. Yu. – Nikityuk D. B. – Gurevich K. G. – Lovtsova L. V. – Kasatkin A. A. – Reshetnikov A. P.: Physico-chemical activity of solutions as an integral part of the mechanism of local action of drugs. Pharmacy. 2019; 68 (6): 43–49. https://doi.org/10/29296/25419218-2019-06-08

[14] Urakov A. L.: The change of physical-chemical factors of the local interaction with the human body as the basis for the creation of materials with new properties. Epitőanyag – Journal of Silicate Based and Composite Materials. 2015;67(1): 2–6. http://dx.doi.org/10.14382/epitoanyag-jsbcm.2015.1.

[15] Shirato M. – Nakamura K. – Kanno T. – Lingström P. – Niwano Y. – Örtengren U.: Time-kill kinetic analysis of antimicrobial chemotherapy based on hydrogen peroxide photolysis against Streptococcus mutans biofilm. Journal of Photochemistry and Photobiology B: Biology, 2017; 173:434-440. https://doi.org/10.1016/j.jphotobiol.2017.06.023.

[16] Urakov A. – Urakova N. – Reshetnikov A. – Kopylov M. – Chernova L.: Solvents of pus-medicines with physical-chemical aggressive action. IOP Conf. Series: Journal of Physics: Conf. Series. 2017;790. – 012033. https://iopscience.iop.org/article/10.1088/1742-6596/790/1/012033/pdf.

[17] Stool Color, Changes in Color, Texture, and Form. Available from: https: //www.medicinenet.com/stool_color_changes/article.htm. [Last accessed on 2010 Feb 5].
[18] Urakov A. L. – Urakova N. A. – Gadelshina A. A.: New medicines: the bleachers of bruises, blue nails, hematomas, blood stains and bloody crusts. Australasian Medical Journal. 2017. V.10, N 11. P. 942 – 943. http://amj.net.au/index.php/AMJ/article/viewFile/3181/1606.
[19] Huang R. – Li M. – Gregory R.L.: Bacterial interactions in dental biofilm. Virulence. 2011; 2(5): 435–444. https://doi.org/10.4161/viru.2.5.16140.
[20] The Chemicals Responsible for the Color of Urine and Feces. Available from: https://www.thoughtco.com/why-is-urine-yellow-feces-brown-606813. [Last accessed on 2019 Jul 8]
[21] How people used to wash: The fascinating history of laundry. Available from: https://thescrubba.com/blogs/news/how-people-used-to-wash-the-fascinating-history-of-laundry. [Last accessed on 2019 Oct 30]
[22] Callewaert C. – Nevel S.V. – Kerckhof F-M. – Granitsiotis M.S. – Boon N.: Bacterial exchange in household washing machines. Front Microbiol. 2015; 6: 1381. https:// 10.3389/fmicb.2015.01381.
[23] Industrial Dyes: Chemistry, Properties, Applications. Edit. K. Hunger. Third, Completely Revised Edition. 2003 WILEY-VCH Verlag GmbH & Co. KGaA, Weinheim. 2003. http://doi.org/10.1.1.674.8611&rep=rep1&type=pdf.
[24] Marzec A.: The effect of dyes, pigments and ionic liquids on the properties of elastomer composites. Polymers. Université Claude Bernard - Lyon I, 2014. English. https://tel.archives-ouvertes.fr/tel-01166530/document. [Last accessed on 2019 Nov 19].
[25] Bleaches. Encyclopedia.com. Available from: https://www.encyclopedia.com/science/news-wires-white-papers-and-books/bleaches. [Last accessed on 2019 Nov 19].
[26] Use of hydrogen peroxide in finfish aquaculture. Available from: https://thefishsite.com/articles/use-of-hydrogen-peroxide-in-finfish-aquaculture.pdf. [Last accessed on 2019 Jan 30].
[27] Italy Is Bleaching Old Seafood to Make It Look Fresh. Available from: https://www.vice.com/en_us/article/gvkmgq/italy-is-bleaching-old-seafood-to-make-it-look-fresh.pdf. [Last accessed on 2019 Aug 14].
[28] Albright RK – White RP.: Red blood cell susceptibility to hydrogen peroxide (H2O2) lysis in chronic hemodialysis patients. Clin Exp Dial Apheresis. 1982; 6(4):223–228. https://doi.org/10.3109/08860228209049855.
[29] Urakov A, – Urakova N.: Rheology and physical-chemical characteristics of the solutions of the medicines. Journal of Physics: Conference Series. 2015; 602: 012043. https://doi.org/10.1088/1742-6596/602/1/012043.
[30] Molenda MA – Sroa N. – Campbell SM. – Bechtel MA. – MD, Opremcak EM.: Peroxide as a novel treatment for ecchymoses. J Clin Aesthet Dermatol. 2010; 3(11): 36-38. Available from: https://www.ncbi.nlm.nih.gov/pmc/articles/PMC2989814/. [Last accessed on 2019 Nov 19].
[31] Lee H.H.B. – Park A-H. – Oloman C.: Stability of hydrogen peroxide in sodium carbonate solutions. Tappi Journal Peer Reviewed Paper. 2000:1–9. Available from: https://docplayer.net/21105316-2000-tappi-journal-peer-reviewed-paper-stability-of-hydrogen-peroxide-in-sodium-carbonate-solutions.html. [Last accessed on 2019 Nov 19].
[32] Hydrogen peroxide: practical, environmentally friendly and antibacterial (2007-2008) Did you know there were so many uses for hydrogen peroxide? Available from: http://www.using-hydrogen-peroxide.com/ [Last accessed on 2019 Jan 30].
[33] Albright RK – White RP.: Red blood cell susceptibility to hydrogen peroxide (H2O2) lysis in chronic hemodialysis patients. Clin Exp Dial Apheresis. 1982;6(4):223–228. https://doi.org/10.3109/08860228209049855.
[34] U. S. Government Printing Office via GPO Access. Code of Federal Regulations, Title 21, Volume 6. Available from: 21CFR582.1366 FDA. [Last accessed on 2019l Jan 30].

Ref.:
Urakov, Aleksandr: *Creation of "necessary" mixtures of baking soda, hydrogen peroxide and warm water as a strategy for modernization bleaching cleaners of ceramic*
Építőanyag – Journal of Silicate Based and Composite Materials, Vol. 72, No. 1 (2020), 30–35. p.
https://doi.org/10.14382/epitoanyag-jsbcm.2020.6

GUIDELINE FOR AUTHORS

The manuscript must contain the followings: title; author's name, workplace, e-mail address; abstract, keywords; main text; acknowledgement (optional)**; references; figures, photos with notes; tables with notes; short biography** (information on the scientific works of the authors).

The full manuscript should not be more than 6 pages including figures, photos and tables. Settings of the word document are: 3 cm margin up and down, 2,5 cm margin left and right. Paper size: A4. Letter size 10 pt, type: Times New Roman. Lines: simple, justified.

TITLE, AUTHOR

The title of the article should be short and objective.

Under the title the name of the author(s), workplace, e-mail address.

If the text originally was a presentation or poster at a conference, it should be marked.

ABSTRACT, KEYWORDS

The abstract is a short summary of the manuscript, about a half page size. The author should give keywords to the text, which are the most important elements of the article.

MAIN TEXT

Contains: materials and experimental procedure (or something similar), results and discussion (or something similar), conclusions.

REFERENCES

References are marked with numbers, e.g. [6], and a bibliography is made by the reference's order. References should be provided together with the DOI if available.

Examples:

Journals:

[6] Mohamed, K. R. – El-Rashidy, Z. M. – Salama, A. A.: In vitro properties of nano-hydroxyapatite/chitosan biocomposites. *Ceramics International.* 37(8), December 2011, pp. 3265–3271, http://doi.org/10.1016/j.ceramint.2011.05.121

Books:

[6] Mehta, P. K. – Monteiro, P. J. M.: Concrete. Microstructure, properties, and materials. *McGraw-Hill*, 2006, 659 p.

FIGURES, TABLES

All drawings, diagrams and photos are figures. The **text should contain references to all figures and tables**. This shows the place of the figure in the text. Please send all the figures in attached files, and not as a part of the text. **All figures and tables should have a title**.

Authors are asked to submit color figures by submission. Black and white figures are suggested to be avoided, however, acceptable.

The figures should be: tiff, jpg or eps files, 300 dpi at least, photos are 600 dpi at least.

BIOGRAPHY

Max. 500 character size professional biography of the author(s).

CHECKING

The editing board checks the articles and informs the authors about suggested modifications. Since the author is responsible for the content of the article, the author is not liable to accept them.

CONTACT

Please send the manuscript in electronic format to the following e-mail address: femgomze@uni-miskolc.hu and epitoanyag@szte.org.hu or by post: Scientific Society of the Silicate Industry, Budapest, Bécsi út 122–124., H-1034, HUNGARY

We kindly ask the authors to give their e-mail address and phone number on behalf of the quick conciliation.

Építőanyag – *Journal of Silicate Based and Composite Materials*, Quarterly peer-reviewed periodical of the Hungarian Scientific Society of the Silicate Industry, SZTE.
http://epitoanyag.org.hu

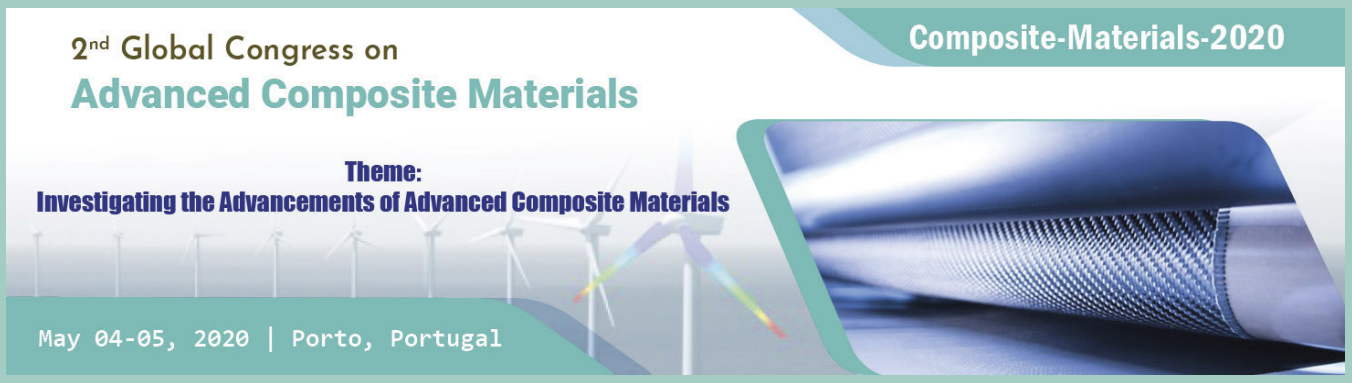

Welcome…!!!

On behalf of the Organizing and Advisory Committee we take great pleasure in welcoming academic scientists, researchers, research scholars, students and experts of application fields to Porto, Portugal for the **2nd Global Congress on Advanced Composite Materials** to foster the progress in the field by contributing with your expertise to what promises to be a very comprehensive and exciting meeting, and to enjoy the immense unique artistic heritage

(Composite Materials-2020), which will be held during May 04-05, 2020 is now an established event, attracting global participant's intent on sharing, exchanging and exploring new avenues of Composite Materials and related research and latest developments. The event will have 5-6 world level (Highly cited class) Plenary speakers, established Keynote speakers, active Invited speakers and fresh contributed speakers. In addition, variety of poster presentations along with workshops and special sessions would be interested in audience.

The aim of the **Composite Materials-2020** is to promote quality research and real-world impact in an atmosphere of true international cooperation between scientists and engineers by bringing together again the world class researchers, International Communities and Industrial heads to discuss the latest developments and innovations in the fields of Composite Materials-2020.

We sincerely hope that **(Composite Materials-2020)** serves as an international platform for meeting researchers from around the world, widen professional contact and create new opportunities, including establishing new collaborations.

Benefits of Composite Materials-2020 conference:

Learn about the latest research in your field

Meet and get to know your peers

Gain visibility in your field

Share your research findings with others in your field

Stay on top of trends and topics

Promote Creativity & Innovation in business field

Global networking In exchanging and trading Ideas

A Unique Opportunity for Advertisers and Sponsors at this International meeting

Grow as a researcher and presenter

Obtain feedback on your research

www.scientificfederation.com/composite-materials-2020/

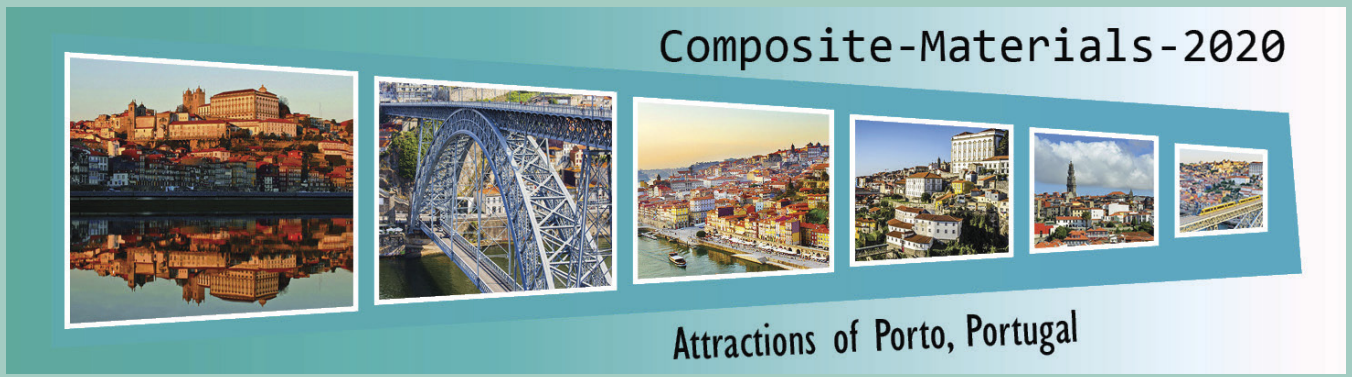

ESCM
EUROPEAN SOCIETY FOR COMPOSITE MATERIALS

THE SCIENTIFIC, ENGIEERING AND INDUSTRIAL COMMNITY INVOLVED WITH COMPOSITE MATERIALS

THE SOCIETY

OBJECTIVES OF THE SOCIETY

ESCM is a European, non-governmental, non-profit scientific and engineering organisation with the following objectives:

- To encourage the free interchange of information on all those aspects related to composite materials which of are interest to the scientific and engineering community.
- To provide a Europe-wide forum for the discussion of such topics, e.g. by organising the ECCM (European Conference on Composite Materials) and more specialised symposia related to composites.
- To guide and foster the understanding and utilisation of the science and technology of composite materials.
- To promote European co-operation in the study of topics in composite materials science and technology.
- To promote liaison with engineering and scientific bodies throughout Europe with similar aims and to serve as a facilitator for communication between such bodies.
- To foster an environment for timely and cost-effective research, development and implementation of advanced technology in composites.
- To encourage the education of young specialists in the disciplines supporting composite materials science and technology.
- To recognise individuals of outstanding achievement in the science, technology, engineering, and application of composite materials.